The Hong Kong Polytechnic University

Department of Applied Biology and Chemical Technology

Structural and biochemical studies of two key components within the autophagy molecular machinery: the Beclin1-VPS34 complex and p62

Liu Wenchao

A thesis submitted in partial fulfillment of the requirements for the degree of Doctor of Philosophy

December 2013

CERTIFICATE OF ORIGINALITY

I hereby declare that this thesis is my own work and that, to the best of my knowledge and belief, it reproduces no material previously published or written nor material which has been accepted for the award of any other degree or diploma, except where due acknowledgement has been made in the text.

Signature:

Name: Liu Wenchao

Dec 2013

Abstract

Autophagy is an evolutionarily conserved cellular pathway that clears long-lived or dysfunctional cytosolic components in response to metabolic stresses and other related signals. The key role of autophagy in maintaining cellular homeostasis leads to its implication in a variety of human disorders. Full understanding of the autophagy process can offer new opportunities for therapeutic intervention of autophagy-related diseases.

Our studies mainly focus on the structural and biochemical mechanisms of two essential components within the complex autophagy molecular machinery, i.e. the p62/SQSTM1 adaptor protein and the Beclin1-Vps34 complex. P62 is a multidomain protein which has been proposed as the adaptor between ubiquitinated proteins and autophagosomes. The issue we seek to address about p62 is to understand the structural mechanism of how the phosphorylation of serine 409 of p62 leads to enhanced association with ubiquitinated protein and its effective clearance by autophagy. The Beclin1-Vps34 complex is the core lipid kinase machinery responsible for the nucleation and maturation of autophagosome. Our work on the Beclin1-Vps34 complex covers two aspects. The first aspect is to understand how the interaction between Beclin1 and UVRAG, an important autophagy modulator, affects Vps34-mediated processes including autophagy and endosomal trafficking. The second aspect is to identify the key structural domains of Beclin1 and Vps34 that are critical for their association to form the Beclin1-Vps34 complex.

For the p62 project we characterized the interaction between p62 UBA domain and mono ubiquitin. Our data reveals that the p62 serine 409 phosphorylation mimic mutant S409E shows about 10-fold stronger binding affinity to ubiquitin than that of wild type. Furthermore, the S409E mutation leads to lower thermal stability, presumably by destabilizing the dimeric form as seen in the wild-type structure. NMR data of the S409E mutant suggests that the S409E mutation leads to conformational changes in p62 UBA domain. Such changes may promote the binding of p62 to poly ubiquitin as in the physiological conditions.

For our study on the Beclin1- UVRAG interaction, our crystal structure of the Beclin1-UVRAG complex reveals a parallel coiled coil with a “perfect” interface consisting of five “leucine-zipper” pairs to render the Beclin1-UVRAG interaction highly stable. Our structure-based functional studies show that this interaction is important for endocytic trafficking like the EGFR degradation but less so in starvation-induced autophagy.

For the Beclin1-Vps34 project we conducted preliminary screening to map the key domains within Beclin1 and Vps34 that are critical for their interaction. Our experiments have uncovered a fragment in the C2 domain of Vps34 that is indispensable for the Beclin1-Vps34 complex association and full activation of the complex. *E.coli* expression system based solubility screening thorough the C2 domain of Vps34 has revealed a soluble but unfolded fragment containing the key Beclin1 interaction region. For future studies, more proper approaches will be

applied to identify the structural and functional features of the Beclin1-Vps34 interaction.

(483 words)

Acknowledgements

I would like to express my sincerely thanks to my principle supervisor Dr Zhao Yanxiang, for her guidance in both academic and personal development. I feel very fortunate and honorable to be one of her research group.

At the same time, I want to thank my co-supervisor Prof. Thomas Leung, who has provided valuable guidance and suggestions to my research project. Especially, I wish to express my deep gratitude to Dr Zhenyu Yue in the department of Neurology, Mount Sinai School of Medicine in USA, for his generous help and supervision in the collaboration with my research work. I also want to thank Dr Lu Jiahong, who provides precious helps in experimental skills and advices in my research work.

I would like to express my deeply thanks to Dr Li Xiaohua, Dr He Yunjiao, Mr Pan Xuehua, Mr Wu Shuai and Ms Sun Lu in our group for their precious helps in experiments and daily life. Meanwhile I also want to thank Dr Cui Wei, Mr Hu Shengquan and Mr Marvin Mark in Prof. Han's group for their earnest helps. And many thanks also give to all the technicians in the department of ABCT, and especially Mr Cheung and Mr Leung for their helps in usage of instruments and facilities.

I also want to express thanks to my parents, my wife Ma Liping and my daughter Liu Mujin. Without their love, encouragement and understanding, I can hardly complete this work.

At last I want to express my acknowledgement to the financial support from the Hong Kong Polytechnic University and the Hong Kong Research Grant Council.

Contents

List of Figures and Tables

List of Abbreviations

Ambra1	Activating molecule in Beclin 1- regulated autophagy
ATG	Autophagy-related genes
Atg14L	Autophagy gene 14 like
Bcl-2	B-cell lymphoma/leukemia-2
BH3	Bcl-2 homology 3
Bif-1	Bax-interacting factor 1
Beclin1	Bcl-2 interaction protein
CCD	Coil-coiled domain
CMA	Chaperone-mediated autophagy
Co-IP	Co-immunoprecipitation
DAP	Death-associated protein
DAPk	DAP-kinase
DSC	Differential Scanning Calorimetry
ECD	Evolutionarily-conserved domain
EGF	Epidermal Growth factor
EGFR	Epidermal growth factor receptor
GFP	Green fluorescent protein
GST	Glutathione-S-transferase
HEK293T	Human Embryonic Kidney 293
IPTG	Iso-propyl thio-galactoside
ITC	Isothermal Titration Calorimetry
LC3	Microtubule associated protein light chain 3
LIR	LC3 interaction region
NMR	Nuclear Magnetic Resonance
PCR	Polymerase Chain Reaction
PI3KC3	Class III phosphatidylinositol 3-kinase
PI3P	Phosphatidylinositol 3-phosphate
SDS-PAGE	Sodium dodecyl sulfate polyacrylamide gel electrophoresis
TOR	Target of rapamycin
Tris	Tris(hydroxymethyl)aminomethane
TRX	Thioredoxin
ULK1	Uncoordinated 51-like kinases
UVRAG	UV irradiation resistance-associated gene
VPS	Vacuolar protein sorting
WT	Wild type

Chapter1 Introduction

Autophagy is a term coined by de Duve more than fifty years ago, coming of the Greek “auto” and “phagy” which means “oneself” and “to eat”, respectively (De Duve and Wattiaux, 1966). Now, it is considered as an evolutionarily conserved homeostatic process in all eukaryotes, in which cytoplasmic components including long-lived and damaged proteins, lipids, sugars, nucleotides, various organelles and invading microorganisms are enclosed into double membrane vesicles and digested by lysosome or vacuole(Cecconi and Levine, 2008; Deretic, 2009; Esclatine et al., 2009; Klionsky, 2005b; Kuma and Mizushima, 2010; Levine and Kroemer, 2008; Mizushima, 2007; Mizushima et al., 2008; Rubinsztein, 2006). Autophagy acts as cellular quality controller not only in the clearance of damaged or long-lived proteins and organelles and but also in the degradation of these intracellular components in normal conditions(Nelson and Shacka, 2013). Furthermore, autophagy also contributes to cellular adaptive response to stressed conditions, such as starvation, serving as an a vicarious source of energy (Singh and Cuervo, 2011). In recent years, mounting reports in the molecular mechanisms of the autophagic process have linked autophagy with the treatment of different diseases and of aging (Mizushima et al., 2008).

1.1 Different types of autophagic pathways

Reports in recent years point out that there are generally three forms of autophagy, macroautophagy, microautophagy and chaperone-mediated autophagy (CMA) based on the different delivery ways of cytosolic components into lysosomes

(Klionsky, 2005b)(Fig 1.1).

CMA is a type of autophagy in which cytosolic proteins labeled by chaperones are captured by a membrane-receptor on the surface of lysosome and subsequently unfolded and directly translocated into lysosomes for degradation(Massey et al., 2004). So far, CMA was firstly revealed in mammalian cells and particularly transports soluble proteins with exposed KFERQ-like motifs to lysosomes. These motifs interact with various chaperones and co-chaperones, such as heat shock cognate protein (hsc70), which help the target proteins bind to the lysosome-associated membrane protein type 2A (LAMP-2A), the receptor on the lysosomal out membrane. Once the destined CMA degradation proteins bind to the lysosome receptor, higher-order molecular complex forms for the intake of target cargo into lysosomes (Kaushik et al., 2011). The last step is the degradation of the cargos in the lysosome lumen and export of the products.

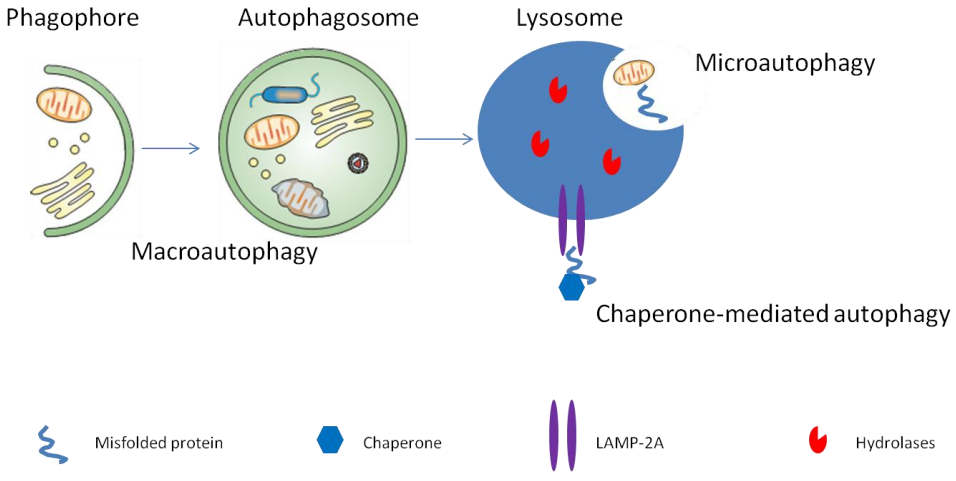

Figure 1. 1 **Schematic pictures of different types of autophagy.**

Microautophagy is the least investigated process, by which the degradative organelles, such as lysosomes or vacuoles, directly intacke cytosolic components by their membranes (Klionsky, 2005a, b). Microautopahgy has only been identified in yeast cells and mainly contributes to the formation and closure of the vacuoles (Sahu et al., 2011; Tuttle et al., 1993). But recent studies describe a microautophagy-like process in mammalian cells, naming endosomal microautophagy. In this process, the complex involved in formation of multi-vesicular bodies has been adopted to construct the invaginating vesicles for the engulfment of cytosolic components to be degraded (Sahu et al., 2011).

The predominant form and the most characterized process, macroautophagy, is identified by the formation of autophagosomes, a kind of double-membrane vesicles which cargo the captured cytoplasmic materials to lysosomes(Klionsky, 2007). Here, in this project, only the macroautophagy, will be called autophagy for short and will be investigated. During autophagy, cytoplasmic organelles and proteins are surrounded by double-membrane structures named phagophore, which is the precursor of autophagosome (Kirisako et al., 1999; Tanida, 2011). Then, the autophagosomes fuse with lysosomes and release cytoplasmic cargos into lysosomes where these cargos are digested by various digestive enzymes. The resulting products including various basic molecules are sent back to the cell cytosol for reuse(Petersen et al., 2014).

Generally, autophagy is in terms of the “in bulk” non-selective degradation of

cytoplasmic components. In recent studies, a series of selective forms of autophagy have also been described. Distinct from the heterogeneous cargos in common autophagy, the autophagosomes in selective forms of autophagy contain single type of cytosolic material. Based on the specific cargos in the autophagosomes, the selective forms of autophagy are named as mitophagy (Goldman et al., 2010; Tolkovsky, 2009), pexophagy (Farre et al., 2009; Veenhuis et al., 2000), recticulophagy (Bernales et al., 2006; Hamasaki et al., 2005), lipophagy (Singh et al., 2009), ribophagy (Kraft et al., 2008) and aggrephagy (Yamamoto and Simonsen, 2011). All these specific forms of autophagy share the same set of critical members of the autophagic regulatory complexes as that in the "in bulk" degradation, and utilize another group of cargo recognition proteins additionally for the specific cargo selectivity. The cargo recognition proteins are described as the adaptors between destined cytosolic components and autophagic machinery. These adaptors are usually multi-domain and multi-function proteins including, p62 and neighbor of BRCA1 (NBR1), (Lamark et al., 2009; Schweers et al., 2007). And heat shock protein hsc70 and BAG-3 have also been indicated to be essential in the selective sorting of aggregated proteins to autophagy pathway (Arndt et al., 2010).

1.2 Molecular signaling of autophagy

Autophagy was firstly depicted in mammalian cells, the knowledge of the autophagic molecular mechanisms mainly came from genetic analysis in yeast, taking advantage of the well established background information in this model

organism (Yang and Klionsky, 2010). From the recognition of the first autophagy-related gene (Atg), *ATG1* (Matsuura et al., 1997) in 1997 to the most recent identification of ATG33 in 2009 (Kanki et al., 2009), totally 33 Atg genes have been uncovered. The protein products of all these Atg genes assemble into different functional machineries regulating autophagic processes: initiation, nucleation, elongation and closure and maturation. In the these processes, there are several core complexes in charge of the critical steps: 1) the Atg1-Atg13-Atg17 complex in the initiation step; 2) the classⅢ phosphatidylinositol 3-kinase (PIK3C3) complex, compose of Vps34-Vps15-Atg6 in the nucleation step; 3) Atg12-Atg5 conjugate and Atg8 conjugate in the elongation step (Fig 1.2)(Wojcik, 2013). Most of the autophagic regulatory investigations concentrate on the nucleation complexes, so do ours. The majority of the yeast Atg proteins have their homologues in mammalian cells, in which these genes usually have much more diverse functions.

Autophagy induction is finely tuned by the regulatory machineries involving various cellular signals, including wide range of stimuli such as starvation, ER stress, mitochondrial damage and signals from the plasma membrane (Klionsky and Emr, 2000; Rabinowitz and White, 2010). In the absence of stimuli, autophagy occurs at a basal level and upgrades greatly after activated. So there should be a system for connecting the extracellular stimuli and the cytoplasmic regulators that directly open the door for autophagy.

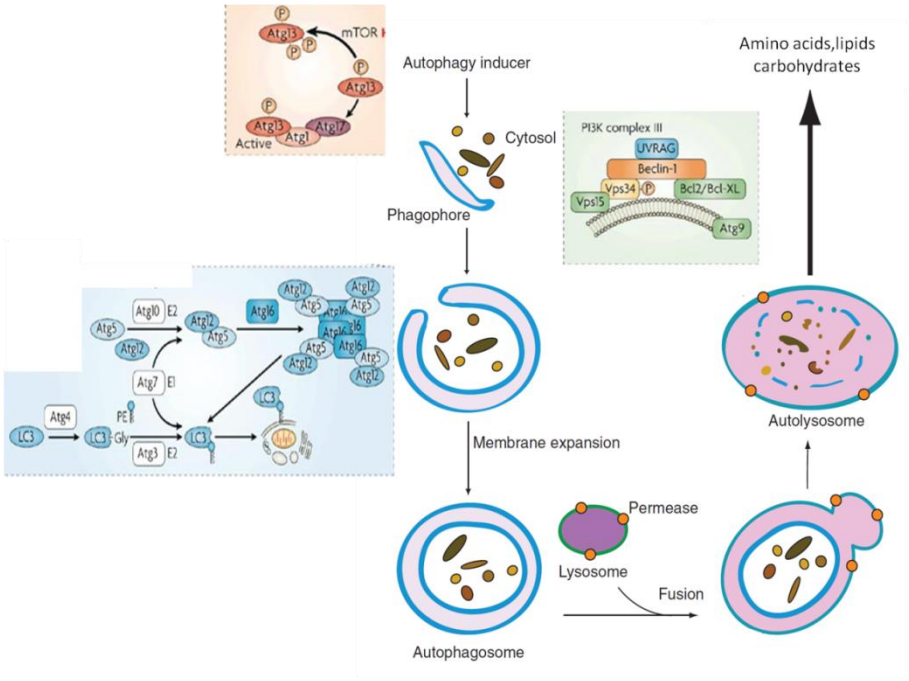

Figure 1. 2 **Overview of the autophagic flux.**

In mammalian cells, mTOR (mammalian target of rapamycin) complex 1 (mTORC1) with serine-threonine kinase activity, which contains mTOR, Raptor (regulatory associated protein of mTOR), mLST8/GβL (G-protein β-subunit-like protein), Deptor (DEP-domain-containing mTOR-interacting protein), and PRAS40 (proline-rich AKT substrate 40KDa), is critical for the initiation of autophagy (Efeyan and Sabatini, 2010; Kuma and Mizushima, 2010). Besides autophagy, mTORC1 mediates diverse cellular events such as proliferation and protein synthesis. Under normal conditions, mTORC1 is activated by class Ⅰ phosphatidylinositol-3-kinase (PIK3C1) and inhibits autophagy initiation via binding and phosphorylating uncoordinated-51-like kinase1 or 2 (ULK1 or ULK2) and Atg13 in the ULK complex (the mammalian orthologs of yeast Atg 1 complex)(Mizushima, 2010). ULK complex contains ULK1/ ULK2, Atg13, FIP200 (focal adhesion kinase

family interacting protein of 200 KDa) and Atg101. In starvation, the kinase activity of mTOR complex 1 is inhibited which frees ULK complex and promotes ULK activity as well as FIP200 hyperphosphorylation(Mizushima, 2010). Then the free ULK1 complex moves from the cytoplasm to specific domain or closely associated structure of ER to recruit the multi-proteins complex (Di Bartolomeo et al., 2010), the PIK3C3 complexes and elongation complexes for vesicle nucleation and autophagosome formation (Itakura and Mizushima, 2010; Mizushima, 2010).

Autophagosome nucleation requires a core complex containing Beclin1 (Bcl-2-interacting protein)—the mammalian homologue of yeast Atg6, p150 (Vps15) and PIK3C3 (Vps34), which further forms larger complexes via binding to additional regulatory molecules such as UVRAG (UV-radiation resistance associated gene), Atg14L and so on (He and Levine, 2010). Recent studies suggest that Beclin1 in the PIK3C3 complex works as the scaffold for the anchoring of interactomes which can mediate the kinase activity of the core complex (Wirawan et al., 2012). The activation of the lipids kinase activity of this complex is required to produce phosphatidylinositol-3-phosphate (PI3P), which interacts with other components such as DFCP1 (double FYVE domain-containing protein1) (Axe et al., 2008) and WIPI (WD-repeat domain phosphoinositide interacting) family proteins (Polson et al., 2010). DFCP1 proteins originally spread on the ER or the Golgi membrane, while they are summoned by PI3Ps to the pre-autophagosome site (PAS) to form ER-associated Ω-like structures termed omegasomes (Axe et al., 2008). The detailed functions of these PI3P interaction molecules need to be illustrated by further

investigations.

Vesicle expansion and completion are the final steps of autophagosome formation in which two ubiquitin-like conjugation systems are indispensable (Tanida, 2011). Firstly, Atg7, the E1-like enzyme activates and brings Atg12 to Atg10, an E2-like enzyme and Atg10 helps the covalent conjugation of Atg12 and Atg5. Next, Atg12-Atg5 core forms trimer with Atg16L1, which further homodimerizes to assemble a large multimeric complex (Kuma et al., 2002; Mizushima et al., 2003). This Atg16L1 complex has been proposed to determine the curvature of the growing autophagosome membrane through transient interaction with the out membrane at the growing point of autophagosome. Secondly, the cysteine protease, Atg4, cut off the C-terminal of LC3 (homologue of Atg8) to reveal a glycine residue. In the combination of Atg7, Atg3 and the Atg16L1 complex, LC3 is covalently linked to phosphatidylethanolamine (PE) finally. LC3-PE or LC3-Ⅱ insert into the membrane of autophagosomes and function as a unique autophagic marker (Kabeya et al., 2004). After the vesicle is sealed, LC-Ⅱ is removed by Atg4 from the outer membrane of autophagosome for recycling.

At the end, autophagosomes are transferred to lysosomes along microtubules. Then, the autophagosomal outer membrane interacts with lysosomal membrane, unloads the inner membrane engulfed cargos into the lysosomal lumen for degradation. Various machineries and proteins have been reported to function in the fusion process, including AAA ATPase, HOPS (homotypic fusion and protein

sorting), ESCRT (endosomal sorting complex required for transport) complex, FYCO1 (FYVE and coiled-coil domain containing 1), LAMP2, LC3, Rab (Ras-related GTP-binding proteins), SNAREs (soluble N-ethylmalemide-sensitive factor attachment protein receptor) and the UVRAG-C-Vps tethering complex (Tong et al., 2010). Interestingly, a type of kiss-and-run fusion has been revealed between lysosome and autophagosome. In this process, the autophagic cargos can be transferred from autophagosome into lysosome while both maintaining separate vesicles (Jahreiss et al., 2008). Once the cargos enter lysosome, the contents are then degraded into carbohydrates, nucleosides, lipids and amino acids which are released into cytoplasm by lysosomal permease system (Yang et al., 2006).

1.3 Autophagy and diseases

Emerging evidences connect autophagy with diverse physiological functions, including cellular energetic balance, protein and organelle quality control, immunity, differentiation and cell death. The alterations in these physiological events often lead to cellular malfunctioning, and set the basis for contributions of autophagy to a wide range of pathogenesis of severe human disorders (Giordano et al., 2014). In these disorders, such as aging, autophagy is basically considered as protective factor, but sometimes also shows the detrimental effects in the progress of some diseases. The dual role of autophagy has been well demonstrated in the pathogenesis and treatment in cancer, heart dysfunction and neurodegeneration diseases as well as immune and infectious diseases.

Autophagy and aging

The general features of aged cells are progressive accumulations of damaged or altered DNA, proteins and organelles and deficits in some physiological processes. Attenuated autophagy activities may play key roles in these events. Bergamini's investigations suggested that autophagy decreased along age, both *in vitro* in isolated liver cells and *in vivo* in rats (Del Roso et al., 2003; Donati et al., 2001). And they also demonstrated that the slowdown of aging by caloric restriction could rescue the attenuation of autophagic activity. In addition, the induction of autophagy by pharmaceutical reagent or starvation improves cellular fitness and longevity of *C.elegans* and *D. melanogaster* (Jia et al., 2007; Mair et al., 2003). In contrast, knockdown or deficiency of key autophagic regulators, such as Beclin1 and Atg7, in *C. elegans* and *Drosphila*, respectively, reduces autophagy activity and the life span of the worms and flies (Juhasz et al., 2007; Melendez et al., 2003). Recent studies on molecular relations between autophagy and aging control imply that diverse cellular pathways and extracellular factors regulate aging via autophagy. Current efforts in rescue the decline of autophagy activity with aging have revealed several potential anti-aging drugs, such as Spermidine and an anti-lipolytic compound (Bergamini, 2005; Eisenberg et al., 2009).

Autophagy and cancer

Through the studies on Beclin1, Levine's group provided the first evidence which connected autophagy with tumorigenesis (Liang et al., 1999). As the

homologue of yeast Atg6 and the core component of the PIK3C3 complex in autophagy, Beclin1 was found to be monoallelically mutated or truncated in the genome of 40-75% human mastocarcinomas, oophoroma and prostate carcinomas(Gewirtz, 2014). And mice with monoallelical Beclin1 deletion in the chromosome accelerate the aggression of spontaneous tumors, such as lung cancers, mammary precancerous, hepatocellular cancers and lymphomas(Gewirtz, 2014). Independent studies reveal deletion of other Atg genes, such as Atg4C, Bif-1 (the Bax interacting factor-1) and UVRAG increase the rate of spontaneous hyperproliferating tumours in mice (Liang et al., 2006; Marino et al., 2007; Takahashi et al., 2007). In the protein level, the autophagy repressors such as Bcl-2, PIK3C1, PKB and TOR, are well known for their tumor-promoting properties, whereas autophagy activators such as PTEN (phosphatase and tensin homolog), DAPK (death associated protein kinase) and TSC1/TSC2 (tuberous sclerosis protein 1/2), are tumor suppressors. The totally opposite effects of autophagy activators and suppressors on tumorigenesis support the tumor suppressive role of autophagy (Mizushima et al., 2008). Furthermore, autophagy has been proposed to inhibit tumorigenesis in the early stages, via its functions in chromosome maintenance and cellular quality control in organelles and proteins. And also, the functions of autophagy in mediating cell cycles contribute to the prevention of spontaneous hyperproliferation (Koneri et al., 2007; Scott et al., 2007). All these evidences indicate the anti-oncogenic functions of autophagy.

However, recent reports indicate that autophagy could also be pro-oncogenic in

certain conditions. Although the mechanisms of the tumor-promoting characteristics of autophagy remain unknown, the most likely hypothesis is that the pro-survival functions of autophagy provide energy and essential materials to tumor cells which surrounded by nutrient poor and hypoxic microenvironments caused by the rapidly growth of tumors (Mathew et al., 2007). It is confirmed by the evidences that the attenuation of autophagy either via genetic deletion or pharmaceutical reagent reduces tumor cell viability during treatment by cancer chemotherapy drugs (Amaravadi et al., 2007). Autophagy has also been found to facilitate Ras-mediating tumorigenesis through its function in maintaining mitochondrial functions and energy levels through facilitating the 'Warburg effect', the unique glucose utilization process used by cancer cells, in which cells prefer to use glycolysis for ATP production (Guo et al., 2011). And its ability to reduce oxidative damage and to maintain the homeostasis of cellular metabolism has also been found to be essential for the proliferation of pancreatic cancers (Yang et al., 2011). The metastasis of tumor cells also requires autophagy to protect them from anoikis after detachment from extracellular matrix (Fung et al., 2008). Mitophagy, the mitochondria specific type of autophagy, has been proposed to be required for the cancer cells transforming via maintenance of highly efficient mitochondria to meet the acute requirement of tumor growth (Guo et al., 2011).

Collectively, the connections between autophagy and cancer development are quite complex and needs to be illustrated further in the future. It has been proposed that the regulation of the two opposite functions of autophagy in cancer strictly

depends on the cell type, disease-context or stage of tumor progression. Due to the complicated relationships between cancer and autophagy, cancer therapy approaches through autophagic pathway should pay special attention to these characteristics. In fact, based on these properties, several autophagic inhibition reagents have been developed and confirmed to be efficient in the cancer therapy, such as oxaloplatin (Ding et al., 2011), sorafenib (Shi et al., 2011), epirubicin (Sun et al., 2011) and 5-fluorouracil (Li et al., 2010).

Autophagy and neurodegeneration diseases

The essential role of autophagy in keeping neuronal health has been well documented in nowadays. Before Rubinsztein's research work on the connections between autophagy and Huntington's disease (Ravikumar et al., 2002), autophagy has been considered to be inactive in neuron cells for the observation of autophagosomes in neuron cells has scarcely been reported. They demonstrated that stimulation of autophagy declined the accumulation of huntingtin aggregates and subsequentially kept flies and mouse models from neurodegeneration. The most compelling evidences come from two independent studies in transgenetically neuron-specific Atg5 or Atg7 knockout mouse models (Hara et al., 2006; Komatsu et al., 2006). These mice exhibit dramatic enhancement in the amount of protein inclusions and neuronal cell decline in their brains. These evidences imply that the absence of autophagosomes in neuron cells could be caused by the high clearance rate of the lysosomes which could rapidly process the freshly generated

autophagosomes. And later, it is reported that the induction of autophagy in nearly all kinds of neuronal cells is beneficial (Webb et al., 2003; Yu et al., 2005). Besides the protective functions in response to general stressors, autophagy is also essential to the defense to neuron injuries, including excitatory toxicity and neuronal ischaemia (Midorikawa et al., 2010; Piras et al., 2011; Rodriguez-Muela et al., 2012).

However, some reports indicate that the attenuation of autophagy during some specific period of post-injury can be beneficial to neuron cells (Cheng et al., 2011). Recent reports also demonstrate that in the case of incapable autophagosome clearance, massive induction of autophagy could become harmful to neurons by permeable leakage of reactive oxygen species from accumulated autophagosomes (Russo et al., 2011).

These findings provide the possibilities of using up-regulation of autophagy as the basis for therapeutic methods for neurodegenerative disease. However, they also remind us the limitation of the widely use of chemical activators of autophagy in treatment of these type of diseases. Firstly, in the scenario that the cellular autophagy machineries themselves have deficits, especially when the clearance of autophagosomes is out of work, stimulation of autophagy could be harmful to cells. For example, in the presence of dopaminergic neurotoxin, LC-II forms abnormal aggregation through interaction with p62. The decline in the amount of LC-II causes failure in response to cell stresses and sequentially incompetency to protect neuron cells (Lim et al., 2011). Secondly, recent findings find that, not all protein aggregates

could be recognized and digested by autophagy, although there is sufficient adaptor or chaperone proteins (Wong et al., 2008). Similar to the cases in the cancer treatment, utilizing autophagy for therapy approaches critically depends on the well understanding of the mechanism behind each type of neurodegenerative disorders. Although it has been well illustrated that autophagy could faciliate the clearance of neuron pathogenic proteins, there are evidences showing that the multiple complexes regulating autophagy are also disturbed in certain diseases. For example, in most forms of Alzheimer's disease, autophagic failures, especially in the clearance steps, are also accompanied (Yu et al., 2005). Similarly, in Parkinson's disease, mutated α-synuclein forms aggregates and interferes in autophagy at the autophagosome formation step (Winslow et al., 2010). Thus, utilization of autophagic modulation for therapy of neuron degenerative disorders requires more studies in the autophagy flux in different types of neuronal disorders.

Autophagy and cardiovascular dysfunction

The first conclusive finding which supports the important role of autophagy in protection of cardiomyocytes is from the genetic model of LAMP-2 knockout mice which exerts dysfunction of heart function and accumulation of autophagosomes in the cardiomyocytes. The mutations in LAMP-2 are found to be the pathogen of human Danon's diseases which demonstrate the similar characteristics as LAMP-2 knockout mice (Lacoste-Collin et al., 2002; Saftig et al., 2001; Tanaka et al., 2000). Furthermore, knockout of Atg5 or Atg7 specifically in cardiomyocyte confirm the

essential roles of autophagy in maintaining normal heart functions both in normal and stressed conditions (Nakai et al., 2007). In the lines of decline of autophagy with age, the age-related cardiomyopathy has also been suggested to correlate with autophagy (Taneike et al., 2010).

Besides the housekeeping functions in normal conditions, autophagy has also been proposed to contribute to the protection of cardiomyocytes in stressed conditions, such as ischaemia-reperfusion injury (Gurusamy et al., 2009; Hamacher-Brady et al., 2006; Huang et al., 2010). Piling evidences support the protective functions of autophagy in cardiac system, especially in the prevention of cardiomyocyte proteinopathies during various cardiac stresses (Tannous et al., 2008; Wang et al., 2001). Because mitochondrial membrane depolarization and ROS produced by damaged mitochondria in stress conditions such as ischaemia-reperfusion are the major cardiomyopathies, autophagy may function in removal of damaged mitochondria and maintenance of efficient mitochondrial function to protect cardiomyocytes from death (Huang et al., 2011; Yitzhaki et al., 2009).

However, some reports point out that autophagy sometimes plays a bad guy in the heart failure. In the specific stage of reperfusion post-ischaemia, induction of autophagy accelerates heart cell death, whereas inhibition provides beneficial effects to heart. It may be explained by the excessive stimulation of autophagy by the huge demand of clearance of damaged organelles and ROS produced in the ischaemia

period and overload of the clearance machinery, kill the cardiomyocytes (Matsui et al., 2007; Zhu et al., 2007). Although these evidences show the opposite functions of autophagy as in cancer and neurodegenerative diseases, in the case under strict control, the activation of autophagy still can be a useful therapy approach for the treatment of heart failure during ischaemia-reperfusion injury.

Autophagy and immunity and infectious disease

There are robust evidences supporting the protective roles of autophagy in prevention of infections by bacteria and virus through a type of selective autophagy called xenophagy (Deretic, 2011). The process of mouth virus and HIV-1 infection and *Streptococcus* Group A invading can induce autophagy which in turn clears these pathogens(Randow and Munz, 2012). Autophagy also acts as a second surveillance point for the pathogens that are able to cheat on phagosomes through engulfing them in autophagosomes and delivering them to lysosomes for degradation (Rich et al., 2003).

However, this mechanism could be utilized by some "smart" pathogens, such as *Porphyromonas gingvalis* and *Coxiella burnetti*, which have been demonstrated to use the autophagosomes for replication and the inhibition of autophagosomal formation decreases the survival of these invaders(Schmid and Munz, 2007). There are some more "cunning" invaders, such as *Staphylococcus aureus*, which has the ability to secret a factor to stimulate autophagy and then uses autophagosomes as shelter and utilizes the cargos inside as energy source (Mestre et al., 2010). As

similar in the previous depicted diseases, use up-regulation of autophagy as therapy strategy needs fully understanding of the characteristics of the pathogenic microorganisms.

Recent studies also connect autophagy with the antigen processing and presentation to lymphocytes in adaptive immunity (Tey and Khanna, 2012). The links are established by the evidences that the block of autophagy flux either by drugs or by genetic manipulations can efficiently attenuate MHC class II intracellular antigen presentation to CD4 T cells (Lee et al., 2010; Nimmerjahn et al., 2003).

Related to the role in the antigen presentation, autophagy has been proposed to function in the establishment of tolerance to self antigens (Starr et al., 2003). The deletion of Atg5 in transplanted thymus causes disorders in the selection and development of autoimmunity (Nedjic et al., 2008). In addition, autophagy activity is required for the sufficient induction of tolerance against self-antigens. The essential roles of autophagy in removal of apoptotic cells connect it to autoimmune diseases which have been proposed to be caused by the failure in clearance of apoptotic cells(Randow and Munz, 2012). It has been observed that the activation of T cells, which is essential for immunity, also requires autophagic activation (Hubbard et al., 2010).

1.4 Regulations on autophagy

For the essential roles of autophagy in human health and diseases, autophagy

has attracted numerous investigations during recent years and a basic schematic for the molecular mechanism in autophagy has been established besides many questions remain in the way to full understanding of autophagy. The most attractive ones are the regulatory mechanisms in the whole process from the induction to the finally fusion with lysosomes, especially the mediations in the nucleation steps (Figure 1.3).

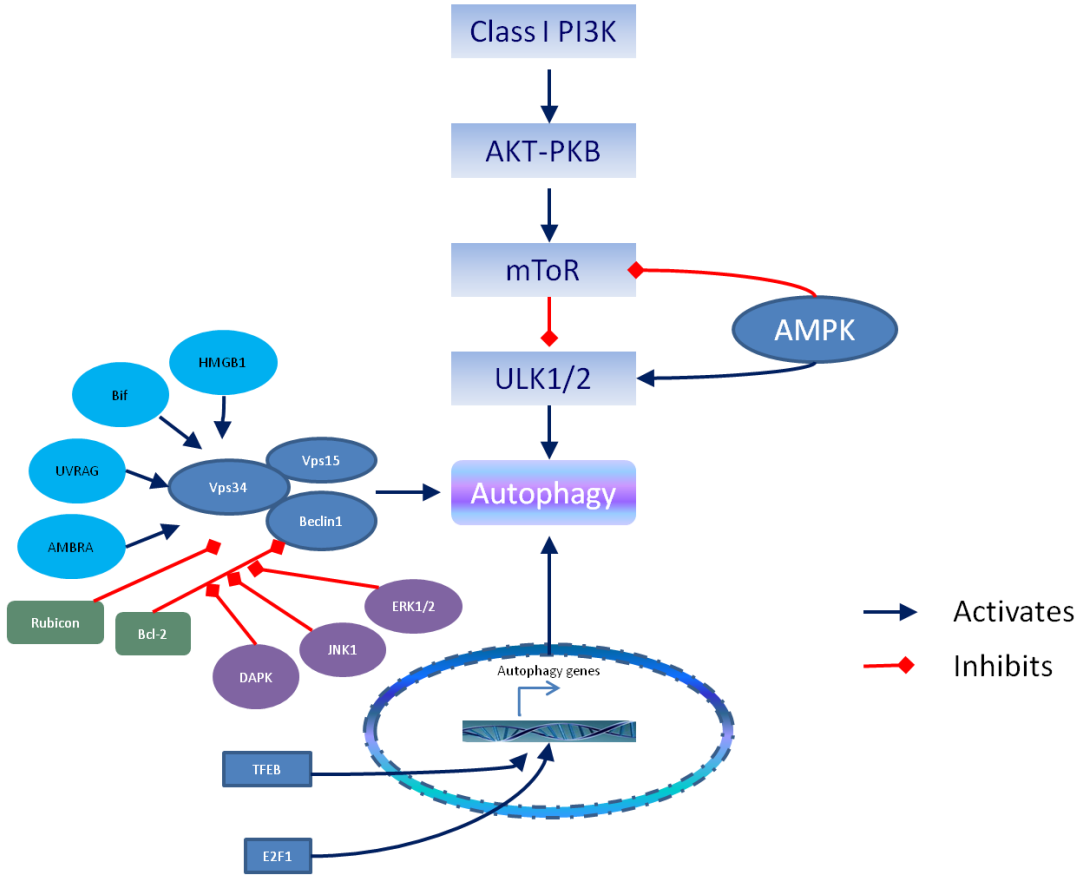

Figure 1. 3 **Regulations of mammalian autophagy.**

In mammalian cells, Beclin1, Vps34 and Vps15 are the core components which exist in various types of complexes by interacting with different binding partners and mainly function in the autophagosome nucleation process (Funderburk et al., 2010; He and Levine, 2010). Some of these binding partners positively regulate autophagy,

such as UVRAG (UV radiation resistance-associated gene) (Liang et al., 2008b), AMBRA1 (activating molecular in beclin-1-regulated autophagy) (Di Bartolomeo et al., 2010; Fimia et al., 2007), Atg14L(Matsunaga et al., 2009; Zhong et al., 2009), and Bif-1 (Bax-interacting factor 1) (Takahashi et al., 2007), while others are negative regulators, such as Rubicon (RUN domain and cysteine-rich domain containing beclin-1-interactong protein) (Matsunaga et al., 2009; Zhong et al., 2009), Bcl-2 and Bcl-xL. These interacting proteins may not only function in autophagy but also in other physiological processes. For example, AMBR1, Bif-1 and UVRAG were found to negatively control growth and suppress tumor progression, whereas Bcl-2 and Bcl-xL are anti-apoptotic members of Bcl-2 family. Most of these multifunction proteins regulate autophagy through directly or indirectly binding to Beclin1-Vps34 complex to activate or repress the kinase activity of the complex and subsequently regulate autophagy (He and Levine, 2010).

Besides these regulatory proteins, autophagy can also be regulated by mediating Atg proteins at both mRNA and protein levels. Activation of the transcriptional factor E2F1 by 4-hydroxytamoxifen up-regulates the protein level of several Atg genes, such as Atg1, Atg5, LC3 and Beclin1 (Polager et al., 2008; Weinmann et al., 2001). Post-translation modifications contribute to the regulation of autophagy in all steps as well. For example, the phosphorylations on Beclin1 and Vps34 alter the interaction between them and sequentially change the autophagic activity (Boya et al., 2013). The details of phosphorylation on Beclin1 and Vps34 will be discussed in the section 1.7 of this chapter. And ubiquitination states of Beclin1 not only affect the stability of

Beclin1 but also control the interaction with Bcl-2 (Wirawan et al., 2012). Calpain-mediated degradation and caspase cleavages also regulate the protein level of Beclin1 and autophagy (Wirawan et al., 2012).

Overall, autophagy plays essential roles in multi-physiological processes of all eukaryotic organisms and correlates to various human diseases. These characteristics invoke us to explore the mechanisms behind the evolutionary conserved processes in the following aspects: 1) p62 phosphorylation driven autophagic selectivity; 2) structure-based functional studies of the UVRAG-Beclin1 complex; 3) structural and functional studies of the Beclin1-Vps34 complex.

1.5 P62 and autophagy

P62, also named Sequestosome-1, is a multi-domain protein which has been reported mediating essential physiological events including bone remodeling, apoptosis, autophagy and tumorgenesis(Rusten and Stenmark, 2010). It was initiately named p62 Lck-ligand for the interaction with the tyrosine kinase Lck (Joung et al., 1996). And the name sequestosome 1 is originated from the functions of p62 to form aggregates and A170 is the original name of mouse p62 (Ishii et al., 1996; Shin, 1998).

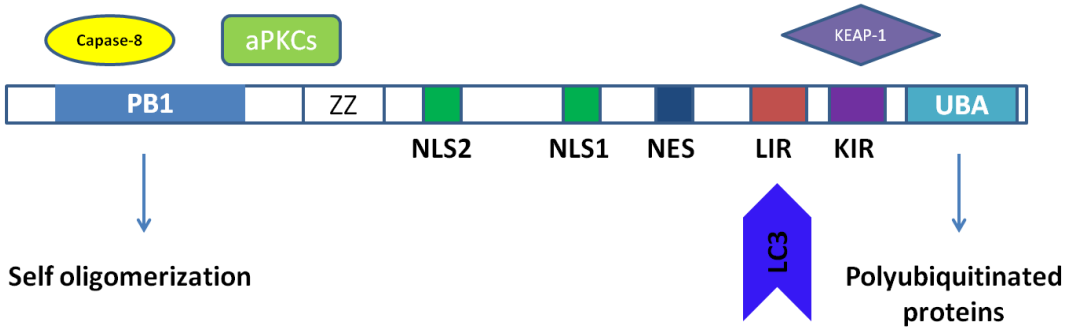

Figure 1. 4 **Schematic representation showing the functional domains of p62.**

The mouse p62 is a 442 amino acids protein which contains a N-terminal PB1 domain, a ZZ-type zinc finger domain, two nuclear localization signal (NLS) motifs, one nuclear export signal (NES) motif, a LC3-interactiong region (LIR) motif, one KEAP1 interacting region (KIR) motif, and a ubiquitin-associated domain (UBA) at the C-terminal (Fig1.4). PB1 domain is a protein-protein interaction domain which is required for the oligomerization of p62 as well as for the interaction with protein kinases PKCs, MEKK3, MEK5 and NBR1 to function in different cellular pathways(Liu et al., 2012). The p62 ZZ (zinc finger motif) domain is in charge of the binding with another binding partner RIP (receptor interaction protein) which harbors aPKCs (atypical protein kinase Cs) to tumor necrosis factor-α (TNFα)-signaling complexes (Sanz et al., 2000). The NLS and NER enable p62 to efficiently shuttle between the nucleus and cytoplasm. The LIR motif is in charge of the interaction with LC3 and is necessary for the autophagic clearance of p62 bodies(Liu et al., 2012). KIR motif has been reported to involve in the regulation of protective responses versus oxidative damages to cellular functional units and biomolecules (Jain et al., 2010). The p62 UBA domain is essential for the ubiquitin binding region

and is also essentially required for its functions in ubiquitinated protein system and autophagy (Cavey et al., 2005; Vadlamudi et al., 1996).

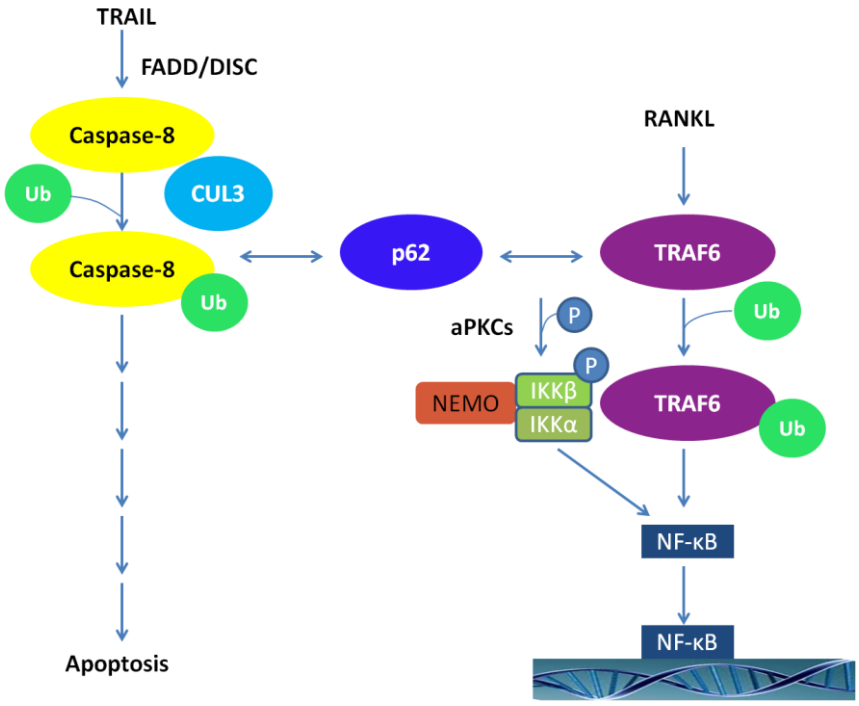

Figure 1. 5 **p62 functions in NF-κB signaling pathway and apoptosis pathway.**

One of the essential roles of p62 is mediating the induction of osteoclastogenesis, which is related to its scaffolding functions in the RANKL-induced NF-κB (nuclear factor kappa B) signaling (Sanz et al., 2000). In the normal conditions, RANKL targets to RANK receptor on osteoclasts, followed by the binding of ubiquitinated TRAF6 to the cytoplasmic domain of RANK. Then, ubiquitinated TRAF6 recruits p62, and aPKCs (atypical protein kinase Cs) binds to the PB1 domain of p62. The atypical protein kinase Cs activate the inhibitor of κB kinase β (IKKβ) in the IKK complex, containing several components, including IKKα, IKKβ, and NEMO (NF-κB essential modulator

or IKKγ). Next, the activated IKK complex phosphorylates the inhibitor of κB (IκB) that makes it K48-linked ubiquitinated and ready for being degraded by proteasomes, followed by releasing of NF-κB. Subsequently, NF-κB relocates to the nucleus and enhances the transcription of selected genes involving in osteoclastogenesis. And P62 may contribute to an alternative way to activate NF-κB by promoting K63-linked ubiquitination of TRAF6. The ubiquitination of TRAF6 activates a complex composed of TAB2 (TAK1 binding protein) and TAK1 (tumor growth factor-β activated kinase1) followed by inducing K63-linked ubiquitination on NEMO. Then, IKK complex is phosphorylated and NF-κB activated (Fig1.5) (Duran et al., 2008). In the p62 knockout mice, the failure of osteoclastogenesis was observed (Martin et al., 2006). And in the patients with Paget diseases, p62 is commonly found to be either with a deletion of the UBA domain or with mutations which are unable to bind to ubiquitin (Laurin et al., 2002). Furthermore, these mutations over-stimulate NF-κB and the osteoclastogenic activity, sequentially lead to excessive bone turnover and bone expansion (Duran et al., 2008) .

There are some findings which link p62 to the extrinsic apoptosis pathway in the full activation of death receptors DR4 and DR5. Cells treated by TRAIL contain promoted polyubiquitination of caspase-8 through a cullin-3-dependent manner (Jin et al., 2009). Then, P62 is recruited to polyubiquitinated caspase-8 and self-oligomerized to trigger the apoptotic pathway (Fig1.5).

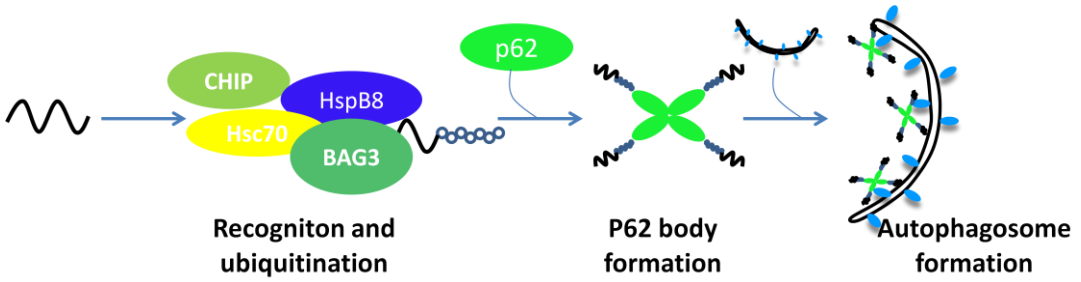

Figure 1. 6 **p62 mediated autophagic degradation of mis-folded proteins.**

As the well known specific substrate of mammalian autophagy, p62 has been considered to be the adapter between autophagosome and autophagy substrates(Liu et al., 2012). This ability has been well depicted by the group of Lipponcott-Swhwartz. They illustrated that p62 was required for recognizing and anchoring the ubiquitinated long-lived protein and peroxisomes to autophagic degradation (Kim et al., 2008). And they also proposed a hypothesis that p62 acted as a linker between substrates and autophagosome. Firstly, the substrates were selectively bound by chaperones and some special cellular molecules and be sorted into autophagic degradation pathway through ubiquitination. Then, p62 was recruited via binding to polyubiquitin and embeds the ubiquitinated proteins into larger aggregates and sequestosomes. Through binding to LC3, p62 recruited the phagophore to sequestered substrates and the autophagosomes formed around the substrates (Fig 1.6). The last step was the fusion with lysosome and degradation of the substrates.

Generally, the ubiquitinated proteins can be cleared up by both the proteasomal and autophagic pathways. It remains unclear if there are specific signals or tags that

selectively lead the substrates either into proteasomal pathway or autophagosomes. Several research groups have reported that p62 UBA domain had a preference to K63-linked polyubiquitin chains compare to K48-linked chains both *in vitro* and *in vivo* (Liu et al., 2012). These results indicate that K48-linked polyubiquitin chain represents a tag for degradation by proteasomal pathway while K63-linked polyubiquitin chain indicates the signal for degradation by autophagic pathway. But it has been pointed out by Nobuyuki Nukina's group that the phosphorylation on p62 plays key roles in the autophagic degradation of polyubiquitinated proteins.

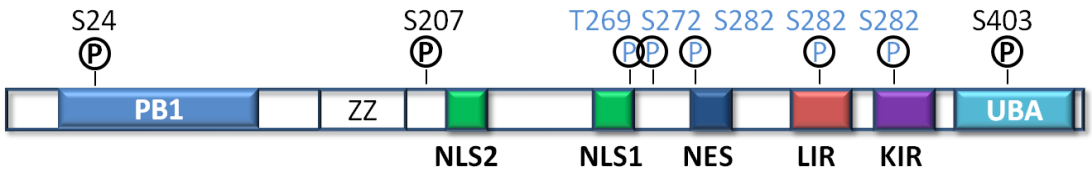

Figure 1. 7 **The phosphorylation sites revealed on p62.** Blue letters indicate constitutively phosphorylated residues and bold letters show the inducible phosphorylation sites.

They revealed that seven serine residues and one threonine residue on p62 were phosphorylated when proteamsomes pathway was inhibited by MG132 (Fig 1.7): S24, S207, T269, S272, S282, S332, S366 and S403. While only S403 in p62 UBA domain was found to be essential for selective binding to the two types of polyubiquitin chains. They demonstrated this phenomenon by generating a phosphor-mimic mutant S403E and a nonphosphorylated mutant S403A and the comparison of their direct binding affinity to two types of polyubiquitin chain *in vitro*. Consistent with previous reports, the wild type and S403A mutant showed

undetectable binding to K48-branched polyubiquitin and significant binding to K63-linked chains. While the S403E mutant bound much more polyubiquitin proteins than that of wild type regardless of K63-linked or K48-linked chains. These findings indicated that the phosphorylation on S403 of p62 significantly promotes the binding affinity to both K48 and K63-linked polyubiquitinated proteins and targets them to autophagosomes without differences. And they also found the phosphorylation increased the formation of sequestosomes and promoted the incorporation of polyubiquitinated proteins into the autophagosomes during proteasome inhibition (Matsumoto et al., 2011). Based on these results, they proposed that the ratio of the S403 phosphorylated p62 and unphosphorylated p62 was a sensor on the level of polyubiquitinated proteins. When the polyubiquitinated proteins increased due to different kinds of cell stress, the balance shifted to the phosphorylated states to sequester the ubiquitinated substrates and followed by autophagic degradation.

Casein kinase 2 (CK2) was found to be in charge of the phosphorylation of p62 S403. Ck2 is identified as a protein kinase that phosphorylates the serine/threonine residues of acidic proteins, such as casein. It plays key roles in a lot of cellular signaling pathways, such as Wnt/β catenin pathway which is essential for the early development, such cell fate determination, embryonic patterning and cell proliferation.

Our collaborator found that the phosphorylation on S409 in the UBA domain of

p62 played a critical role in the degradation of ubiquitinated proteins by autophagy. Furthermore, the phosphorylation enhanced the interaction between ubiquitinated proteins and p62. Our aim in this part of work is to provide structural interpretation for the increased interaction between p62 and ubiquitinated proteins.

1.6 UVRAG and UVRAG containing complex

UVRAG, the ultraviolet radiation resistance-associated gene, was firstly identified in KCL22 myeloid leukemia cells and named by its capacity to providing UV resistance in *Xeroderma pigmentosum* cells (Perelman et al., 1997). It contains several functional domains: a proline-rich (PR) domain at N-terminal, C2 domain and CCD domain in the middle, with a large C-terminal end. The PR domain is related to the binding of Bif, which positive regulated the kinase activity of UVRAG containing Vps34 complex and played a role as tumor suppressor (Takahashi et al., 2007). And the C2 domain has been reported to be a binding domain of several signaling molecules, including Vps16 in the class C vacuolar protein sorting (Vps) complex (Liang et al., 2008b), Bax in the proapoptotic group of Bcl-2 protein family (Yin et al., 2011) and PtdIns(3)P which is essential in endocytic, phagocytic and autophagic pathways (He et al., 2013). The CCD domain is mainly in charge of binding to Beclin1 to form a UVRAG-Beclin1-Vps34-Vps15 complex functioning in autophagic and endocytic pathway(Song et al., 2014). The long C-terminal domain is proposed to bind to RINT-1, a member of the ER tether complex (He et al., 2013), and also interacts with two important binding partners in maintaining the stability of

chromosome: CEP63 and DNA-PK complex (Zhao et al., 2012a; Zhao et al., 2012b). Through binding to distinct partners, UVRAG participates in diverse cellular trafficking events (Fig 1.8).

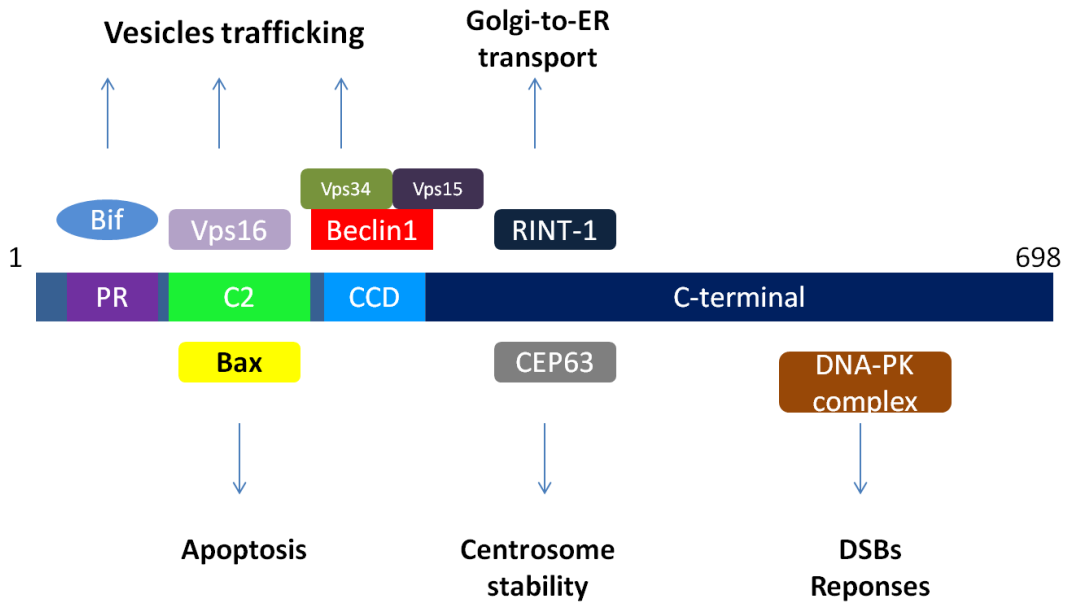

Figure 1. 8 **UVRAG and its binding partners.** DSBs: DAN double-strand breaks.

In 2006, UVRAG was reported to form complex with the Beclin1-Vps34-Vps15 autophagic machinery via interaction with the CCD domain of Beclin1. It is the first report that indicated UVRAG as a Beclin1 binding partner, which can increased the contacts between Beclin1 and Vps34 and the kinase activity of Vps34 complex. And also, the binding of UVRAG to Beclin1 has been proposed to be indispensable for the formation of autophagosome and tumor suppression in HCT116 and MCF7 cell lines. Stably over expression of UVRAG in NIH3T3 cells increased basal, rapamycin and starvation induced autophagy, while knockdown of UVRAG by siRNA in HeLa cells considerably decreased the formation of autophagosome (Liang et al., 2006). However, recent evidences suggest that the main job of UVRAG is not in autophagy

induction. In 2008, Mizushima's group demonstrated that the UVRAG siRNA treated HeLa cells showed significantly decrease in UVRAG protein level, while no observed reduction in starvation induced autophagy in terms of LC3 conversion, p62 degradation and autophagosome formation (Itakura et al., 2008). Later, another report also indicated that there was no obvious relationships between the amount of UVRAG and the activity of autophagic pathway in several cell lines including HCT116, RKO, LoVo, HCT115 and HEK293T (Knaevelsrud et al., 2010). These contradictory results render the role of UVRAG in autophagy debatable and further studies are needed to resolve this controversy.

In addition to Beclin1, UVRAG also has another binding partner Vps16, which is one of the components in the core class C Vps complex functioning in the fusion of multiple vesicles, including endosomes, lysosomes, autophagosomes and so on. It is proposed that there are two separate sites for Vps16 binding on UVRAG, the C2 domain and a region from residue 270 to 442 in the C-terminal domain, and each of them is sufficient for binding to Vps16. Stable overexpression of UVRAG in HeLa cells enhances the fusion of autophagosome and lysosome, or the autophagosome maturation. And also UVRAG-C Vps complex plays essential roles in the endocytic trafficking through promoting the endosome-endosome fusion. Beclin1-UVRAG interaction was proposed to be genetically separated from the functions in the autophagosome maturation and endocytic pathway (Liang et al., 2008b). But later, a Norwegian research group found that not only UVRAG, but also Beclin1-Vps34-Vps15 complex and bif-2 play key roles in the EGFR degradation

and endocytosis (Thoresen et al., 2010). This report provides opportunities for further investigation on Beclin1-UVRAG interaction in the endocytic pathway.

Besides the autophagy and endocytic functions, UVRAG has been illustrated to be very important in many other cellular processes. It is reported that UVRAG suppresses apoptosis through blocking the mitochondrial translocation of Bax (Yin et al., 2011). UVRAG is also playing key roles in maintaining chromosomal stability. With binding to the DNA-dependent protein kinase, UVRAG engages in the nonhomologous end joining process, which is a preferential path to rejoin the broken DNA ends in mammalian cells in responding to DNA double-strand breaks (DSBs) (Zhao et al., 2012a; Zhao et al., 2012b). UVRAG is required for centrosome stability and effective chromosome segregation through binding to centrosome protein CEP63 (Zhao et al., 2012a). Recently, UVRAG is revealed to be required in the Golgi-to-ER transport and cis-Golgi integrity through the interaction with RINT1-ZW10-NAG ER tether complex and Ptdlns(3)P (He et al., 2013).

In this part of study, we are trying to look closely into the interaction between Beclin1 and UVRAG by resolving the crystal structure of the complex. Furthermore, we are aiming to reveal Beclin1-UVRAG interaction mediated functions, especially in autophagy and endocytosis.

1.7 Beclin1-Vps34 complex

Beclin1 is the mammalian homologue of yeast Atg6/vacuolar protein sorting

(Vps)30 protein and it was firstly identified as a Bcl-2 interaction protein(Kang et al., 2011). It contains three independent functional domains: a Bcl-2 homology (BH)-3 domain, a central coiled coil domain (CCD) and an evolutionally conserved domain (ECD) (Kang et al., 2011). BH3 domain of Beclin1 is in charge of binding to Bcl-2 and other anti-apoptotic proteins. The CCD domain is in charge of the interaction with Ambra1 (activating molecule in Beclin1-regulated autophagy), UVRAG and Atg14L (Fimia et al., 2007; Itakura et al., 2008; Li et al., 2012). Together with CCD domain, ECD domain interacts with PI3KC3/Vps34 (Fig 1.9) (Liang et al., 2006).

Vps34 is an evolutionally conserved phosphoinositide (PI) 3-kinase from yeast to mammalian cell (Vanhaesebroeck et al., 2010). It was firstly cloned as a protein involving in the protein sorting to the vacuole in *Saccharomyces cerevisiae* (Jaber et al., 2012). Yeast only contains one type of PI 3-kinase, Vps34, but mammalian cells has several Vps34 homologues and they can be categorized into three classes by the substrates specificity and the resulting products (Vanhaesebroeck et al., 2010). Vps34 contains an N-terminal C2 domain, a central helical domain in the middle and end by the catalytic domain. The C2 domain is proposed to interact with Beclin1, the helical domain and catalytic domain form the catalytic core, and a region composed of 46 residues is required for the interaction with Vps15 (Jaber et al., 2012). Through interacting with Vps15 and Beclin1, Vps34 forms a core complex which functions in different cellular trafficking events. In yeast, the Vps15-Vps30-Vps34 core complex is involved in at least two essential signaling pathways, autophagy and vacuolar protein sorting, through forming larger complexes with Atg14 and Vps38

respectively (Jaber et al., 2012). In mammalian cells, Beclin1-Vps34-Vps15 core complex also exists in two distinct complexes via binding to Atg14L and UVRAG correspondingly. Atg14L-containing complex mainly regulates the autophagy pathway and UVRAG-containing complex plays key roles in both autophagy and endocytic pathway(Bechtel et al., 2013). The interrelationship of these two mutually exclusive Beclin1-Vps34-Vps15 containing complexes remains unknown (Li et al., 2012).

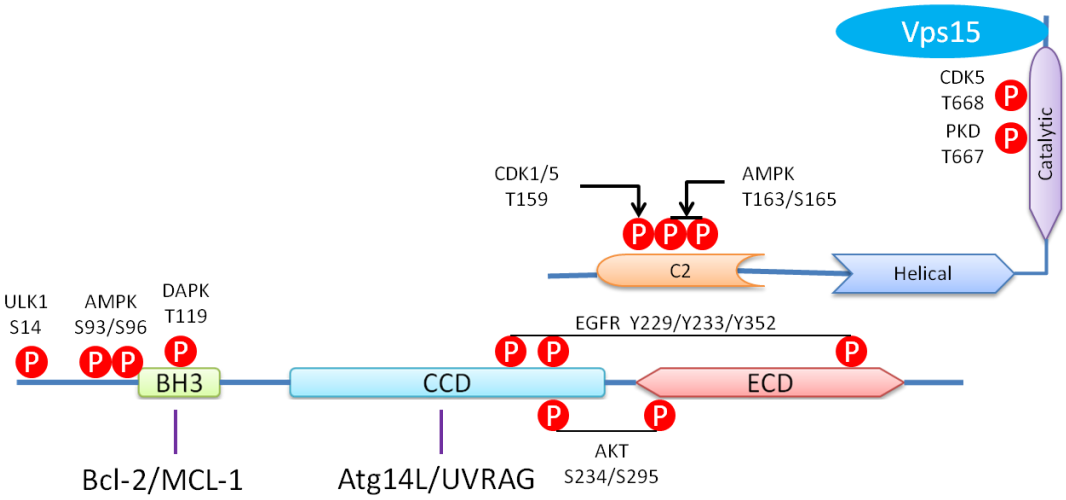

Figure 1. 9 **Schematic picture of the phosphorylation sites on Beclin1 and Vps34.**

The essential roles of the Beclin1-Vps34 complex in the regulation of multiple signaling pathways have attracted mounting investigations on the interaction between them. The anti-apoptotic proteins such as Bcl-2, Bcl-xL, Bcl-w and Mcl-1, have been reported to negatively regulate the interaction between Beclin1 and Vps34 through interaction with the BH3 domain of Beclin1 (Germain et al., 2011; Maiuri et al., 2007; Pattingre et al., 2005). And RUBICON (run domain Beclin1-interacting and

cysteine-rich containing protein) and NLRP4 (nucleotide-binding and oligomerization domain like receptor 4) bind to the ECD domain of Beclin1 and diminish the Vps34-Beclin1 complex formation (Jounai et al., 2011; Wei et al., 2013; Zhong et al., 2009). The Beclin1-Vps34 interaction can be interfered by viral proteins, such as the viral homologues of Bcl-2 from several γ-Herpes-viruses (Liang et al., 2008a) . In contrast, Ambra1 activates autophagy in a way stabilizing the association of Becin1 and Vps34 (Fimia et al., 2007).

Other than the binding partners, the post-translation modifications, especially phosphorylation on these two molecules, has been revealed to play essential roles in the interaction of these two molecules and the activity of the complex (Fig 1.8). Furuya and co-workers found that Thr^{159} in the C2 domain of Vps34 was phosphorylated by CDK1 (cyclin dependent kinase 1) and CDK5 between metaphase and anaphase in cell cycle and resulted in the disruption of Beclin1 binding and autophagy inhibition. They also found that Thr^{668} in the catalytic domain of Vps34 was also phosphorylated by CDK5 and the kinase activity was decreased (Furuya et al., 2010). Another paper described that Vps34 was activated during ROS induced autophagy with phosphorylation of Thr667 by protein kinase D (PKD) (Eisenberg-Lerner and Kimchi, 2012). Recently, a report illustrated that AMPK phosphorylated the Thr163 and Ser165 by in the C2 domain of Vps34 and played a role in the inhibition of non-autophagic Vps34 complex's kinase activity during glucose starvation (Kim et al., 2013).

Beclin1 has also been considered as the substrate of various kinases during autophagy. The phosphorylation of Beclin1 has been related to the interaction with Vps34 as well. As reported by Zalckvar and colleagues, DAPK directly phosphorylated Thr119 in the BH3 domain of Beclin1 and released Beclin1 from Bcl-xL, subsequentially increase the Beclin1-Vps34 interaction (Zalckvar et al., 2009). And ROCK1 (Rho kinase 1) functions in the same way by disrupting the Beclin1-Bcl-2 interaction (Gurkar et al., 2013). Levine's group demonstrated that overexpressed Akt decreased the Beclin1-Vps34 interaction via phosphorylation of Ser^{234} and Ser^{295} of Beclin1 (Wang et al., 2012). A recent report showed that Beclin1 was phosphorylated at three tyrosine sites (Tyr^{229}, Tyr^{233} and Tyr^{352}) in the ECD domain by activated EGFR and attenuated Vps34 binding (Wei et al., 2013). The phosphorylation of Ser^{14} by ULK1 and $Ser^{91/94}$ by AMPK were proposed to increase the kinase activity in the Atg14L-containing Beclin-Vps34 complexes via introducing conformational changes in Vps34 (Kim et al., 2013; Russell et al., 2013).

Although there are extensively studies on the interaction between Beclin1 and Vps34, but the evidences for the physical interaction between these two molecules are missing. And even the exact boundaries of the interaction domains on these two proteins are not available. Our studies in this part are trying to find some clues for the direct interaction between Beclin1-Vps34 and this interaction related functions.

Chapter2 Materials and Methods

2.1 Plasmids construction

All the wild type plasmids were constructed by general cloning procedure: amplification of target DNA fragments by polymerase chain reaction (PCR), digestion by restriction enzymes and ligation with expression vectors, transformation and sequencing after digestion screening. The cloning related reagents and enzymes were bought from Thermo Scientific.

The mutant plasmids including deletion, truncation and point mutation were conducted based on the wild type plasmids using site-directed mutagenesis as depicted in the protocol provided by the manufacture of Phusion Site-Directed Mutagenesis Kit (Thermo Scientific).

In the p62 project, the UBA domain (residues 391-438) of mouse p62 protein was cloned into the modified pET49 vector (Novagen) between the restriction sites BamHⅠand EcoRⅠ. The full length of mouse ubiquitin was inserted into the modified pET32 vector between the restriction sites BamHⅠand EcoRⅠ. For dimer exchange assay, UBA domain of p62 was cloned into the pRSETa vector with His_6 at amino terminal but without protease 3C cutting site. And the mutants S409A/E were cloned to the same vector.

In UVRAG-Beclin1 interaction studies, constructs aimed at protein purification were prepared using the modified pET32 vector (Novagen) which containing a thioredoxin-6XHis tag and a protease 3C cutting site in the upstream of multi-clone

site. The DNA fragments corresponding to the coding sequence of the peptide 228-275 of mouse UVRAG and 174-223 of Beclin1 were linked by the DNA sequence of tandem of 5Xglycine-serine repeats using PCR. The linked DNA fragment and the corresponding individual fragments were cloned into the expression vector pET32M between the restriction sites BamHⅠand EcoRⅠ. For the transient expression in mammalian cells, the DNA sequences of full length mouse UVRAG and Atg14L were cloned into both pEGFP-N3 vector and pcDNA3.1 (Invitrogen) derivative vector containing an N-terminal Flag epitope tag. And the DNA sequences of mouse Beclin1 were amplified and cloned into pCMV-myc vector between EcoRⅠand XholⅠsites.

In Beclin1-Vps34 interaction studies, all the solubility screening constructs were prepared using the modified pET based vectors (Novagen) which containing thioredoxin-6XHis tag (pET32m), 6XHis tag (pETm), GST-6XHis tag (pET49m) or MBP-6XHis tag (pMBP) respectively and a protease 3C cutting site in the upstream of multi-clone site. Vps34 constructs were inserted between BamHⅠand XholⅠ and the Beclin1 constructs were between BamHⅠand EcoRⅠ. The 5XGS linked constructs were obtained using the similar strategy as in the UVRAG-Beclin1 studies. For the transient expression in mammalian cells, the DNA sequences of full length mouse Beclin1 and Vps34 were cloned into both of pEGFP-N3 and pCMV-myc vectors (Clonetech).

2.2 Protein expression and purification

The expression plasmids were transformed into the *Escherichia coli* BL21 (DE3) cells and induced by 0.2-0.5mM IPTG at 16-30℃ for 6hrs. The proteins were then purified by His-trap column and Hiload Superdex75 16/60 on the AKTA Purifier system (GE Healthcare) following the manufacturer's instructions. Briefly, induced bacteria were lysed in His-binding buffer (20mM sodium phosphate buffer, pH7.4, 40mM imidazole) by sonication. After 2hrs centrifugation at 20000rpm, the supernatant was loaded onto the His-trap column followed by 10 column volume His-binding buffer wash. The target proteins were separated from the affinity tag by protease 3C and further purified by the size exclusion chromatography. His tagged p62 UBA samples used in dynamic exchange assays were prepared without tag removing step. The N^{15} labeled samples were prepared by growing cells in M9 minimal media containing $^{15}NH_4Cl$ (6g/L Na_2HPO_4, 3 g/L KH_2PO_4, 0.5g/L NaCl, 2mM $MgCl_2$, 0.1mM $CaCl_2$, 1g/L $^{15}NH_4Cl$, 2g/L Glucose).

2.3 NMR spectra collection

All the ^{1}H-^{15}N HSQC spectra of wild-type and mutant p62 UBA domain were collected at a concentration of 100μM protein in 20mM sodium phosphate buffer, pH6.8, 5mM potassium chloride, 1mM EDTA and 10% D_2O. For the ubiquitin titration, 6-equimolar ubiquitin was mixed with the ^{15}N labeled UBA samples before the data collection. The spectra were acquired with a Bruker Avance 700 MHz spectrometer and data were processed by the software provided by the manufacture.

The ^{1}H spectrum of Vps34 C2J fragments and the ^{1}H-^{15}N HSQC spectra of

linked C2J and Beclin1 were collected by the same machine but in a protein concentration of 0.5mM in PBS buffer at pH7.4.

2.4 Isothermal titration calorimetry (ITC)

A MicroCal VP-ITC$_{200}$ was used to perform all the ITC related experiments and data processing was conducted with the software Origin 7 provided by the manufacture. All the protein samples used in ITC were prepared in buffer containing 50mM Tris-HCl, pH8.0 and 150mM NaCl. To acquire a high quality profile, all the protein samples and buffers were filtered and degassed prior to the data collection. At least three independent titrations of each experiment were performed.

For the determination of ubiquitin binding constants of different p62 UBA mutants, 2μl of 1mM ubiquitin was injected at 180s intervals into the cell containing 50μM UBA samples(Wild-type, S409A and S409E) at 25℃. For the UBA dimer dissociation constants, 500μM UBA samples were loaded in the syringe and titrated to the blank buffer in the same set up in ubiquitin binding experiments. Generally, titrations consisted of 20 injections.

To measure the binding constants between UVRAG mutants and Beclin1 wild type peptide, 2μl of 1mM UVRAG peptides was injected at 180s intervals into the cell containing 50μM Beclin1 peptide, or 1mM Beclin1 peptides were titrated in to UVRAG mutated peptides in the same setting as in p62 UBA-ubiquitin binding.

2.5 Differential Scanning Calorimetry (DSC)

In the thermal stability tests of p62 UBA, DSC measurements were carried out by a MicroCal VP-DSC calorimeter with 0.5ml cells under a constant pressure of 2.5 atm. For the thermal stability data collection, all the protein samples were exchanged to buffer containing 20 mM HEPES, pH7.4, 115 mM NaCl, 1.2 mM $CaCl_2$, 1.2 mM $MgCl_2$ and 2.4 mM K_2HPO_4 by dialysis. Five rounds of buffer to buffer scans from 10-90℃ by a ratio of 60℃/hr were performed to acquire a high quality baseline and a consistent thermal history prior to the protein data collection. The protein samples at a concentration of 200μM were degassed and warmed to 25℃ before being loaded to the sample cell. All the protein samples were injected in a temperature window between 15-25℃ when the cell cooling down to 10℃ after the previous scan. Data were analysis by the software provided by the manufacture (MicroCal, Inc), including baseline subtraction, normalization and model fitting. For each experiment, at least three independent scans were performed.

2.6 Dynamic Exchange Assay

In p62 UBA dynamic exchange assays, His_6-tagged and untagged same type (wild type/S409A/S409E) p62 UBA domains were mixed and incubated together in ~ 1:2 molar ratio at different temperatures for 20 min in 250 μl exchange buffer (150 mM NaCl, 50 mM Tris buffer, pH 8.0, 40 mM imidazole) to form heterodimer. Pre-equilibrated Ni^{2+}-NTA agarose beads were added to samples, rolling in 4℃ for 30min, then centrifuged to co-precipitate Ni^{2+}-NTA beads with bound protein complexes. Bound protein complexes were eluted by elution buffer after thoroughly

wash, and equal volume of elutant was analyzed by SDS-PAGE.

2.7 Immunoprecipitition and western blotting

All the cells were grown in Dulbecco's Modified Eagle's medium (DMEM) containing 10% fetal bovine serum and 1% penicillin-streptomycin (Invitrogen). Transient transfection was conducted with Polyjet DNA intro transfection reagent following the manufacture's protocol.

Cells were collected 24 hours after transfection, followed by being lysed in magnesium containing lysis buffer (MLB) composed of 25 mM HEPES (pH 7.5), 150 mM NaCl, 10 mM $MgCl_2$, 1 mM EDTA, 1% Nonidet P-40, 1% Triton X-100, 2% glycerol, and protease inhibitor cocktail (Roche Diagnostics). After being clarified by centrifugation at 10000g for 10 min, total protein concentrations were determined by Bradford kit (BioRad) and 500-1000μg total proteins containing lysate were subjected to IP. All the lysates were normalized to 1μg/μl prior to adding 10μl 50% slurry ANTI-FLAG M2 Magnetic Beads or 2μg specific antibodies together with protein A/G agarose (Santa cruz) into each sample. After incubation at 4℃ for 2 hours, beads were thoroughly washed with lysis buffer and eluted by SDS reducing dye via boiling for 10 min.

For immunoblotting, samples were resolved by SDS-PAGE and transferred to PVDF membrane (GE Healthcare). Immunodetection was performed with anti-Flag (1:1000) (Sigma), anti-Beclin1 (1:500) (Santa Cruz Biotech), anti-GFP (1:1000)

(Roche), anit-c-myc (1:1000) (Roche), anti-EGFR (1:1000) (Santa Cruz Biotech), anti-LC3 (1:1000) (MBL), anti-p62 (1:1000) (ARP). The bands were visualized by SuperSignal West Pico Chemiluminescent substrate (Thermo).

2.8 EGFR degradation

Twenty four hours after transfection, cells were washed with PBS and serum starved overnight in DMEM containing 20mM HEPES. EGF (200 ng/ml) was added to stimulate EGFR endocytosis. Then, cells were collected at each time point and lysed in MBL buffer. Equal amounts of cell lysate were analyzed by SDS-PAGE and followed by detection of EGFR using western blotting.

2.9 Autophagy assays

Autophagy was induced by starvation. Cells were washed two times with PBS 24 hours after transfection and incubated in Earle's balanced solution (EBSS; Invitrogen) for 2 hrs at 37℃. The cells were collected and subjected to western blotting for detection of p62 and LC3.

2.10 *In vitro* Vps34 Kinase activity assays

The IP samples of Vps34-Beclin1 complexes were washed once by kinase assay buffer (20 mM HEPES, pH7.4, 1 mM EGTA, 0.4 mM EDTA, 5 mM $MgCl_2$) and then were incubated with KA buffer containing 50uM cold ATP, 5mM $MnCl_2$, 50 μM DTT, 0.1 mg/ml phosphatidylinositol and 5 μCi ^{32}P-ATP for 30 min at 37℃ for 30

min with frequent shaking. The reactions were stopped by $CHCl_3/CH_3OH/HCl$ (10:20:0.2) mixture and continuously shaken for 10 min. After centrifuging at 6000g for 5 min, 15 μl of the lower phase samples were separated by a thin-layer-chromatography (Whatman) under $CHCl_3/CH_3OH/NH_4OH/H_2O$ (86:76:10:14) mixture. And radioactive signals were detected by autoradiography (GE Healthcare).

Chapter3 Results

3.1 Biochemical and structural characterization of p62/SQSTM1 – ubiquitin interaction and the impact of Serine 409 phosphorylation on this interaction

Our collaborator, (Dr. Zhenyu Yue's lab in Mt. Sinai School of Medicine, New York, NY U.S.A.) has found that ULK1 phosphorylates p62 at residue S409 within the UBA domain. Such phosphorylation leads to enhanced association of p62 to ubiquitinated proteins and is critical for effective protein degradation by autophagy if the proteasomal pathway is inhibited (manuscript under preparation). Our aim here is to investigate, through biophysical and biochemical methods, how the S409 phosphorylation in p62 leads to enhanced association with ubiquitinated proteins. Based on previous reports on the dimer structure of p62 UBA domain and its incompatibility with ubiquitin binding, we hypothesize that the phosphorylation of S409 leads to destabilization of the auto-inhibited p62 UBA dimer conformation and facilitates more effective ubiquitin binding.

3.1.1 p62 UBA-ubiquitin interaction can be enhanced by phosphorylation–mimicking mutant S409E

For our *in vitro* studies we have focused on the p62 UBA domain. This domain, where residue S409 is located, is directly responsible for ubiquitin binding. We have generated three p62 UBA constructs, including the wild type and two mutants S409E and S409A. The S409E mutation is meant to mimic the phosphorylation event and S409A mutation is to represent the absence of phosphorylation. All these three UBA

constructs were expressed and purified to homogeneity following standard procedures.

The first biochemical assay we performed was Isothermal Titration Calorimerty (ITC). Our aim is to compare the binding affinity of these three constructs to mono ubiquitin. The K_d for wild-type p62 UBA is ~100 μM, confirming a generally weak interaction between p62 UBA domain and mono-ubiquitin. The K_d for phosphorylation-mimicking S409E mutant is ~10 μM, nearly 10 times stronger than that of wild-type. Furthermore the K_d for phosphorylation-deficient S409A mutant is ~300 μM, slightly weaker than that of wild-type and about 30 times weaker than that of S409E (Fig. 3.1.1). These data suggest that the side chain property of residue 409 exerts noticeable impact on the binding affinity of p62 UBA domain to mono-ubiquitin, with charged or polar side chain groups favorable to this interaction while hydrophobic side chains unfavorable.

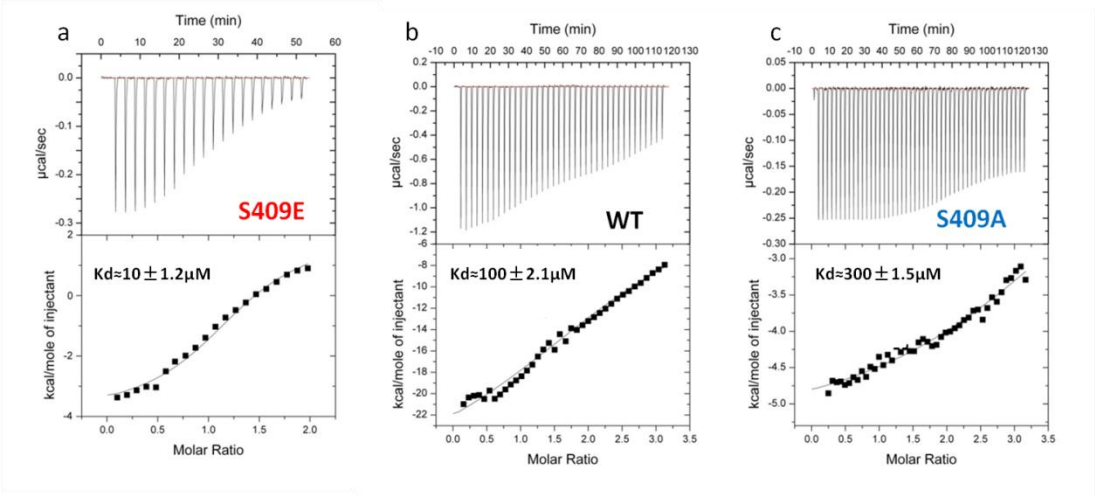

Figure 3. 1. 1 **S409E mutation increases its binding affinity to ubiquitin.** ITC titrations with ubiquitin

in the syringe and S409E (a), WT (b) and S409A UBA in the cell. The data were fitted to single site models.

3.1.2 S409E mutation destabilizes p62 UBA homodimer

1) Dynamic exchange assay

Firstly, dynamic exchange assays were performed to study the stability of the p62 WT, S409E and S409A UBA dimers. Both His-tagged and untagged UBA domains were co-incubated at the indicated temperatures and pulled down by Ni^{+} NTA agarose beads after cooled on ice for 5 minutes, followed by examination by SDS gel. If there is dynamic exchange among p62 UBA dimer molecules, the pull-down sample would contain both the Hig-tagged and untagged samples with noticeable mass difference of ~1 kDa. In fact our data show that for all three constructs, the eluted sample contained almost exclusively His-tagged protein only, suggesting that little dynamic exchange occurred over the wide temperature range of 22 – 70 ^{o}C (Fig 3.1.2). These findings suggest that the *in vitro* dimeric form of p62 UBA domain is highly stable. Single-residue mutations like S409E or S409A, although close to the dimer interface, do not lead to significant impact on the overall thermostability of the dimer interface. Our result is consistent with the previous report that p62 UBA dimer is stable in aqueous solutions (Isogai et al., 2011).

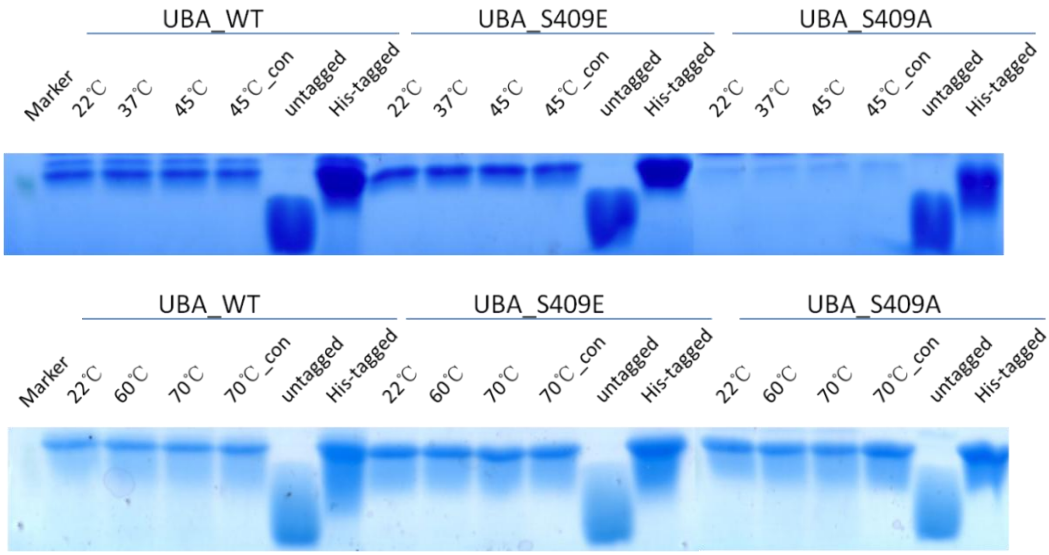

Figure 3. 1. 2 **UBA dimer undergoes little dynamic exchange in solution.** Dynamic exchange assays of wild type, S409E and S409A p62 UBA domain at temperature from 22℃ to 70℃.

2) Probing dissociation of p62 UBA domain by ITC experiments

To further characterize the thermostability of p62 UBA dimer, ITC was applied to determine the dissociation constants of wild type p62 UBA and two mutants. Our experimental data of the dissociation constants among the three types of p62 UBA revealed that WT had the highest dimer stability (K_d = 8.5±1.7 μM), S409A in the middle (K_d = 12±2.9 μM) and S409E at the lowest (K_d = 40±1.4 μM). (Fig3.1.3). The much weaker dimer stability of S409E is in general agreement with our hypothesis.

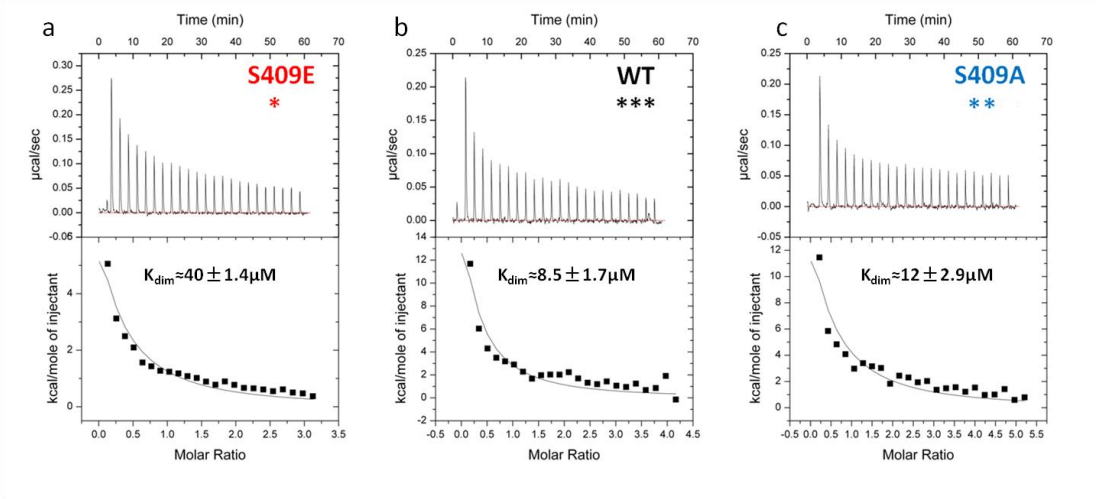

Figure 3. 1. 3 **S409E mutation reduces UBA dimer stability.** Dimer dissociation assays with buffer in cell and S409E (a), WT (b) and S409A (c) UBA in syringe. The data were fitted to dissociation models. The number of "*" roughly represent the stability of UBA dimer.

3) DSC profile, thermal stability of the p62 UBA domain

Next, to support these findings, we applied differential scanning calorimetry to determine the thermal stability of p62 UBA dimer. The thermal stability of the mutants and WT p62 UBA domain was assessed by Differential Scanning Calorimetry (DSC). The T_m of S409E was determined to be 61.5±0.01℃, which is about 4℃ lower than that of the wild-type at 65.8℃. And the T_m of S409A was at 59.6℃, which is even lower than that of S409E (Fig 3.1.4). The lower T_m of S409E as compared to WT indicates that the phosphorylation-mimicking S409E mutation leads to reduced thermal stability of p62 UBA domain, in support of our hypothesis. However the lower T_m of S409A as compared to WT is inconsistent with our hypothesis as this mutation is expected to strengthen dimer stability. Furthermore *in vivo* data from our collaborator's lab shows weakened binding for S409A to

ubiquitinated proteins. The inconsistency of the DSC data probably reflects the limitation of this method, rather than disapproving our hypothesis. For one thing, it is possible that the T_m measured in DSC does not correlate directly with the dimer stability as the two processes of the dimer dissociation and protein denaturation might be convoluted in the process of heating during DSC procedure. Secondly DSC method is highly sensitive to calibration and buffer conditions etc. We need to conduct more vigorous control experiments, like multiple buffer-to-buffer measurements, to ensure the DSC data are robust.

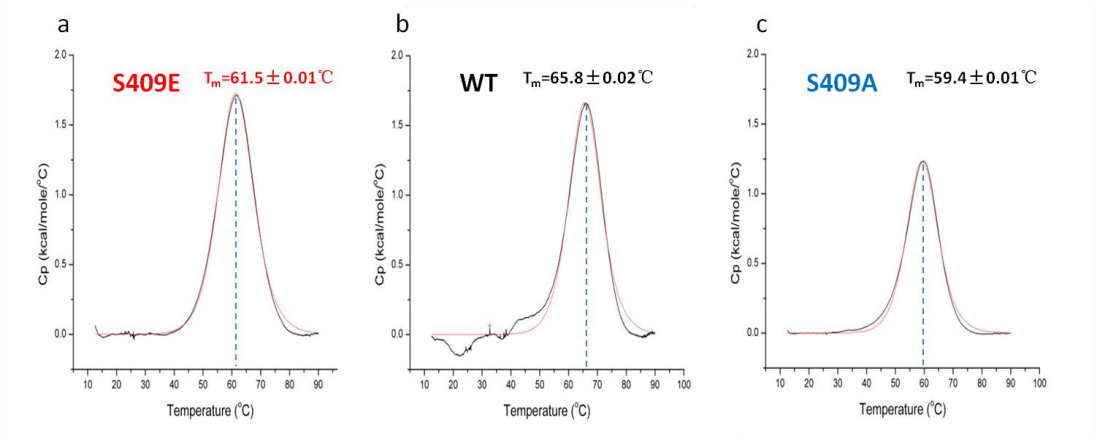

Figure 3. 1. 4 **DSC profile of p62 UBA constructs.** DSC profiles of S409E (a), WT (b) and S409A (c) at a protein concentration of 200μM and a heating rate of 1℃/min from 10℃ to 90℃. The data were fitted to non-two states models.

4) NMR analysis of p62 UBA

Next, NMR studies were carried out to investigate the structural profile of p62 UBA S409E.

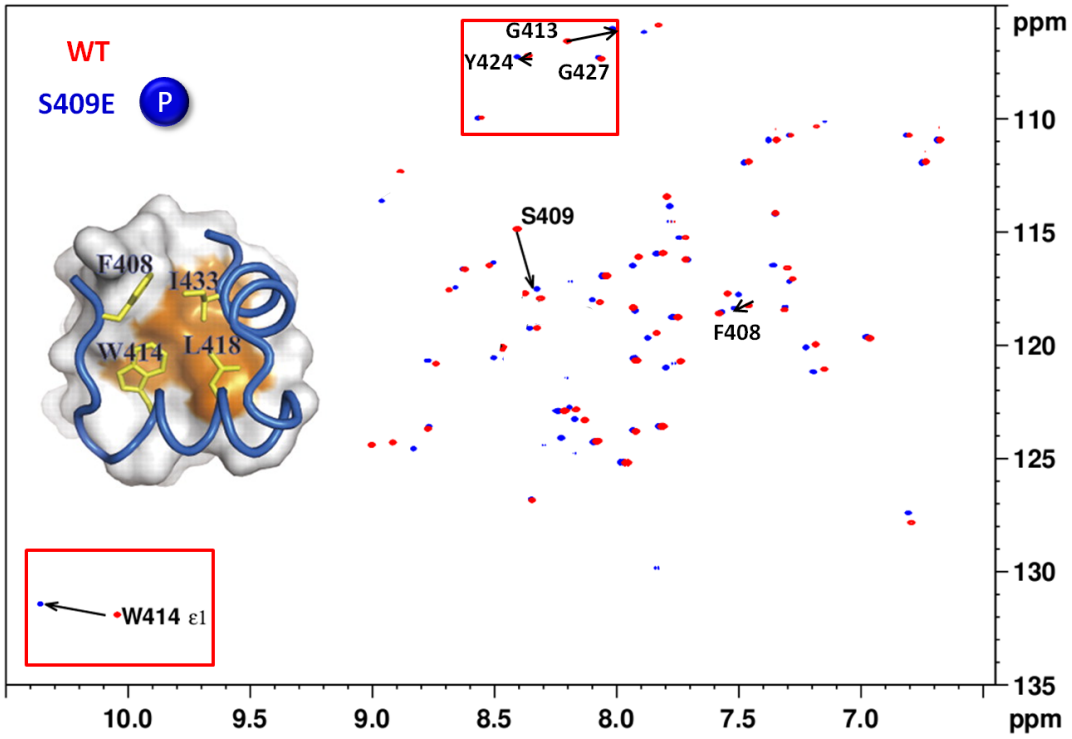

Figure 3. 1. 5 **S409E mutation causes conformational changes on UBA dimer interface and ubiquitin binding motif MGF.** The overlay of ^{1}H-^{15}N HSQC spectra of ^{15}N-labeled WT (red) and S409E (Blue) UBA at concentration of 100μM. Cross-peaks in the red rectangles represent the residues critical for the dimer interface.

The ^{1}H-^{15}N correlation spectra of the ^{15}N-labeled p62 UBA wild type and S409E mutant were first collected in the absence of ubiquitin (Fig. 3.1.5). The overall disperse pattern of cross peaks for S409E mutant is largely identical to that of wild-type. A few chemical shifts are significant and the corresponding residues D410, G412, W414 and L418 were identified using the published wild-type spectra as reference. All these residues are located in the vicinity of residue 409 and it is logical that the S409E mutation alters their local environment and leads to chemical shift in the HSQC spectra. Noticeably residues W414 and L418 are both important

constituents of the UBA dimer interface in the wild-type structure. The chemical perturbation caused on these residues by S409E mutation may lead to destabilization of the dimer interface.

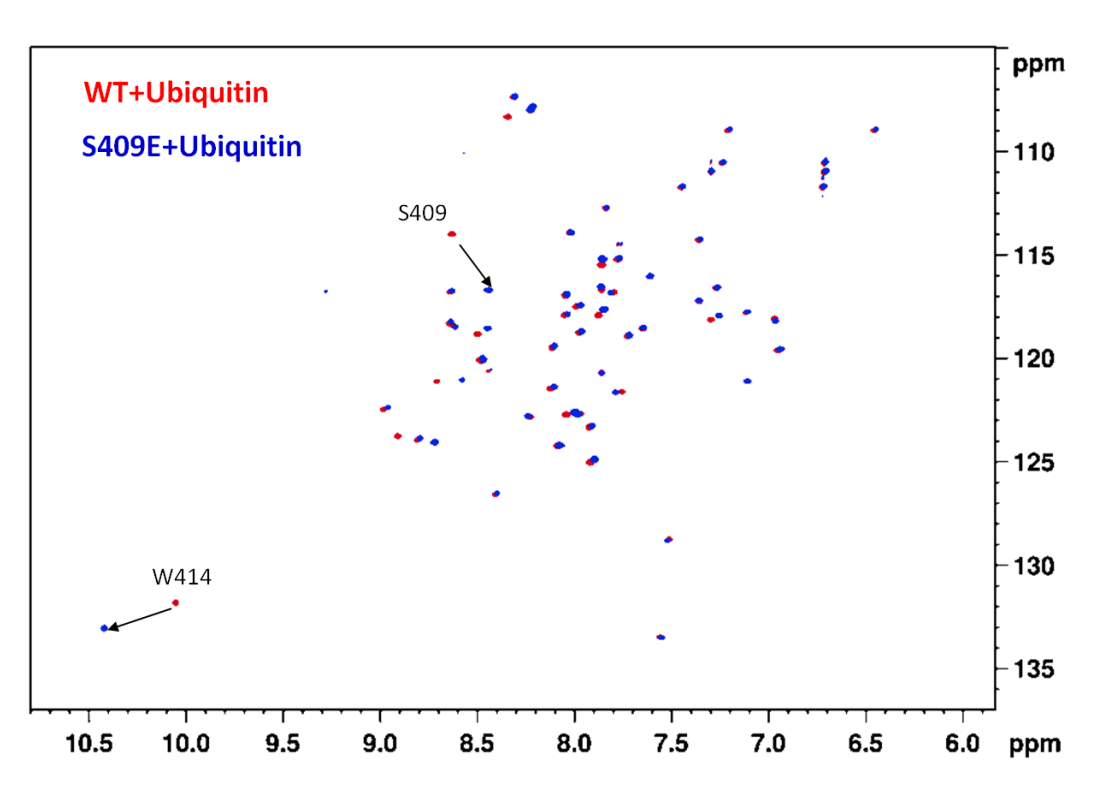

Figure 3. 1. 6 **S409E binds to mono-ubiquitin similarly to WT.** The overlay of ^{1}H-^{15}N HSQC spectra of ^{15}N-labeled WT (red) and S409E (Blue) UBA at concentration of 100μM in the presence of 600μM native mono-ubiquitin.

NMR titration experiments were carried out by adding 6-fold molar excess of unlabelled mono-ubiquitin to the wild-type and S409E mutant UBA proteins. First of all the addition of mono-ubiquitin induced a large set of chemical shifts in the spectra of S409E mutant, confirming that S409E undergoes the dimer-monomer transition upon ubiquitin binding as reported in previous studies for wild-type p62 UBA domain. Close inspection reveals that the disperse pattern of S409E in presence of

ubiquitin is also largely similar to that of wild-type, with only a few noticeable chemical shifts involving residues such as S409E and W414. These data suggest that S409E mutant interacts with mono-ubiquitin in highly similar manner to that of wild-type, with the S409E mutation exerting little influence (Fig. 3.1.6).

3.2 Structure-based functional studies of the UVRAG-Beclin1 complex

This part of work is focused on functional study of the UVRAG-Beclin1 interaction by focusing on two processes it mediates: autophagy and endocytosis. We first aim to determine the crystal structure of the UVRAG-Beclin1 complex. Based on the crystal structure, we then proceed to conduct structure-based functional studies to explore the essential cellular roles of UVRAG-Beclin1 interaction using site-directed mutagenesis, ITC and co-immunoprecipitation.

3.2.1 Crystal structure of Beclin1-UVRAG complex

A polypeptide containing residues 174-223 of mouse Beclin1 at the N-terminal, the residues 228-275 of mouse UVRAG at the C-terminal and a 5X(GS) linker in the middle, was expressed, purified and crystallized (Fig 3.2.1a). The UVRAG-Beclin1 complex structure was determined at 2.0 Å resolution. This structural study was carried out by Dr. Yunjiao He, my fellow labmate. It is included here to give a more comprehensive description of the Beclin1-UVRAG project.

The peptides from two proteins form a canonical parallel coiled coil heterodimer which is distinct from the anti-parallel homodimer of Beclin1 CCD domain (Fig 3.2.1c) (Li et al., 2012).

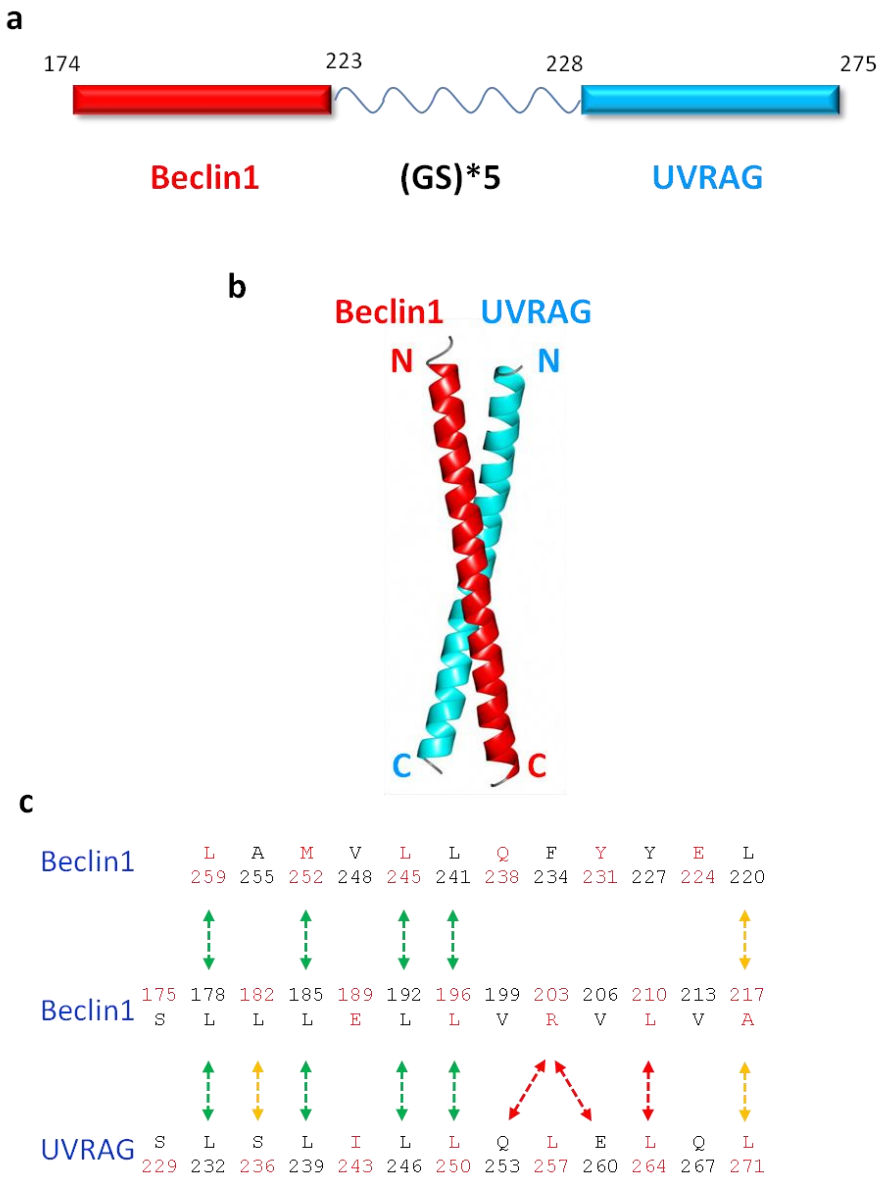

Figure 3. 2. 1 **Crystal structure of Beclin1-UVRAG complex**. (a) The schematic picture of the linked complex in crystal. (b) The parallel dimeric coiled coil structure of the Beclin 1-UVRAG complex. (c) Comparison of the coiled coil interface of Beclin 1 homodimer and the Beclin 1-UVRAG heterodimer. Green arrows mark the strongly hydrophobic “leucine zippers”; Yellow arrows mark the moderately hydrophobic pairings and red arrows mark the stabilizing pairings only observed in Beclin 1-UVRAG complex. (Note: the crystal structure of Beclin1-UVRAG complex is resolved by Dr He Yunjiao in our group).

The Beclin1-UVRAG dimer interface contains five “leucine-zipper” pairs that are formed between the leucine residues (L178, L185, L192, L196 and L210) of Beclin1 and the corresponding leucine residues (L232, L239, L246, L250 and L264) of UVRAG. In addition to the hydrophobic “leucine zipper” pairs, the positively charged side chain of R203 in Beclin1 forms a salt bridge with the negatively charged side chain of E260 and a hydrogen bond with the polar side chain of Q253 in UVRAG (Fig 3.2.1c). The hydrophobic “leucine zippers”, together with the charge complementary salt bridge and hydrogen bond underlie the extraordinary strong affinity of the Beclin1-UVRAG interaction.

3.2.2 Key residues identification in UVRAG-Beclin1 interaction *in vitro*

Using the Beclin1-UVRAG complex as guidance, we generated a series of UVRAG mutations to confirm the key residues in the Beclin1-UVRAG interaction. Based on the structural information of the complex, we substituted the hydrophobic “L” residues on UVRAG indicated by arrows in Figure 3.2.1C with negatively charged “E” or replaced the negatively charged 260E with positively charged “R”. This *in vitro* study was carried out by Dr. Yunjiao He, my fellow labmate. It is included here to give a more comprehensive description of the Beclin1-UVRAG project.

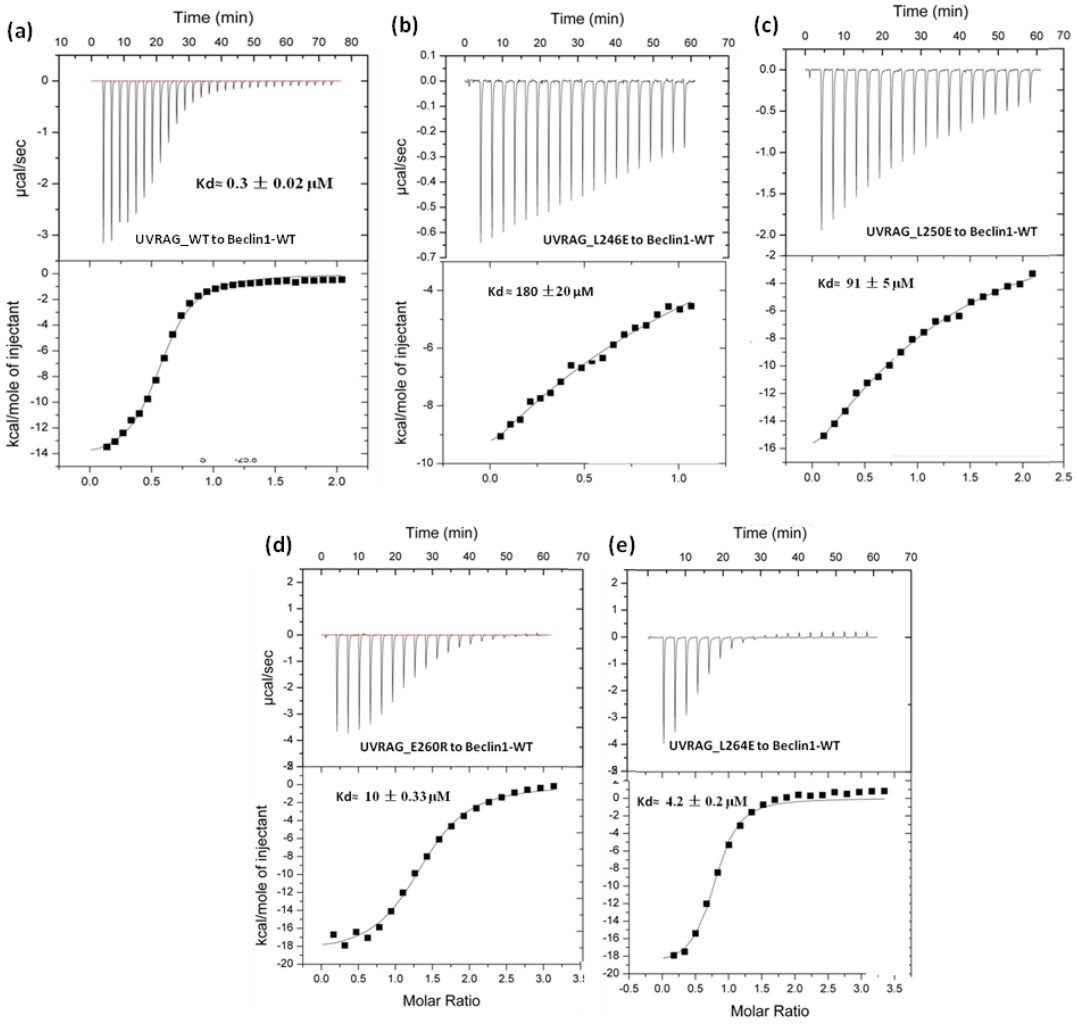

Figure 3. 2. 2 **UVRAG single mutations reduce their affinity to Beclin1**. ITC titrations with UVRAG wild type or mutants in syringe and Beclin1 (174-223) in cells. The data were fitted to single site models.

Firstly, we generated four single-site UVRAG mutants (L246E, L250E, L264E and E260R) aiming to weaken or abolish Beclin1-UVRAG interaction. Next, we determined the binding affinity between UVRAG mutants and Beclin1 by ITC. The K_d for wild type UVRAG is ~0.3μM, confirming a strong interaction between Beclin1 and UVRAG. The K_d for L246E is 180μM, for L250E is 91μM, for E260R

is 10μM and for L264E is 4.2μM (Fig3.2.2). Although the single mutations on UVRAG showed dramatically decreased binding affinity to Beclin1 by almost two orders of magnitude as compared to that of wild type, these single mutants still retained weak interactions with Beclin1. These data suggest that the strong Beclin1-UVRAG interaction can not be abolished when a single residue is mutated at the dimer interface. Furthermore, the differences of the affinity to Beclin1 among the UVRAG mutants suggest different weightings of these residues in maintaining the interaction.

Since the single site mutations were not strong enough to abolish the interaction between Beclin1 and UVRAG, we constructed several multiple sites mutations including one double mutant (L246E_L250E), a triple mutant (L232E_L239E_L271E), a penta mutant (L232E_L239E_L246E_L250E_L264E) and a hexa mutant (L232E_L239E_L246E_L250E_L264E) and investigated their interactions with Beclin1 by ITC as well. All the multi-site mutants show a titration profile that suggests little or no interaction between Beclin1 and these UVRAG mutants (Fig 3.2.3). These data confirm that removing multiple leucine residues within the Beclin1-UVRAG interface is sufficient to abolish their interaction.

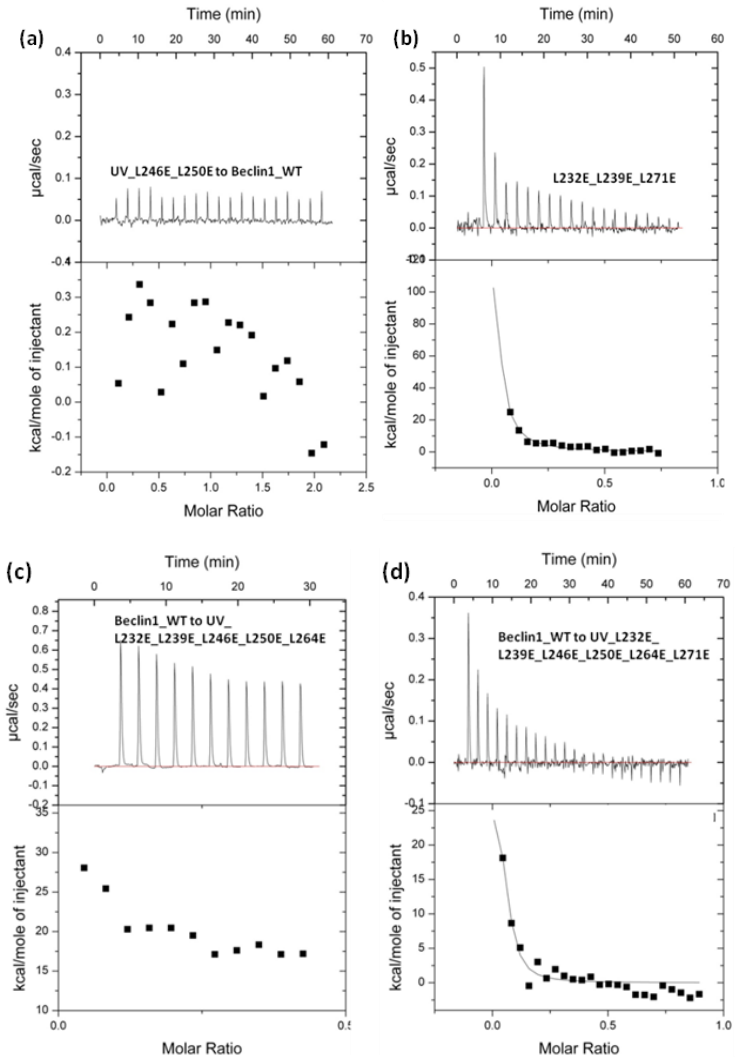

Figure 3. 2. 3 **UVRAG multi-sites mutants lost interaction with Beclin1.** ITC with UVRAG mutants in syringe and Beclin1 (174-223) in cell. (Note: The *in vitro* interaction studies is done by Dr He Yunjiao in our group)

3.2.3 Key residues identification on UVRAG-Beclin1 interaction *in vivo*.

The crystal structure of the Beclin1-UVRAG complex and the *in vitro* studies have identified a group of key residues for their interaction. Next, we performed co-immunoprecipitations in HEK293T cells to confirm these findings *in vivo*.

Firstly, we studied the interactions between Beclin1 and the UVRAG mutants that have lost interaction with Beclin1 as shown by ITC experiments. We transfected the Flag tagged full length UVRAG mutants including a single mutant (L246E, for control), a double mutant (L246E_L250E), a penta mutant (L232E_L239E_L246E_L250E_L264E) and a hexa mutant (L232E_L239E_L246E_L250E_L264E) mutants separately into HEK293T cells. Twenty four hours after transfection, cell lysates were immunoprecipitated by anti-Flag magnetic beads and the immunocomplexes were analyzed by western blotting using anit-Beclin1 antibody. As shown in Fig 3.2.4, Beclin1 can be detected in the pull-down fraction by all the UVRAG mutants. These data indicate that when over-expressed *in vivo*, these UVRAG mutants still retain interaction with Beclin1.

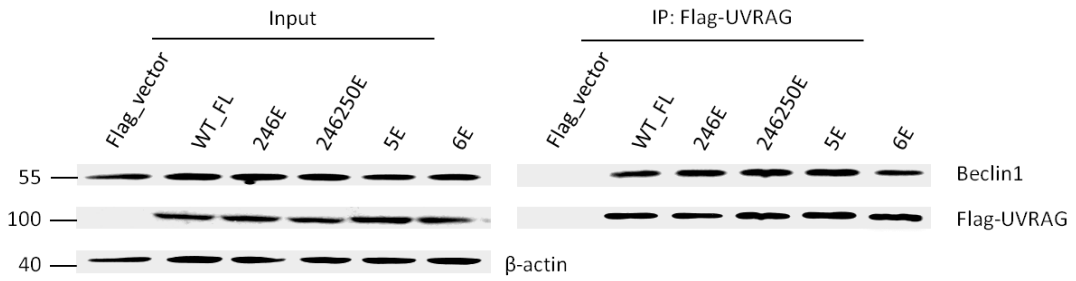

Figure 3. 2. 4 **All the mutations retain interactions with Beclin1.** HEK293T cells were transfected with Flag-UVRAG mutants plasmids. Twenty four hours after transfection, cell lysates were immunoprecipitated by anti-Flag magnetic beads and the immunocomplexes were analyzed by western blotting using anit-Beclin1 antibody.

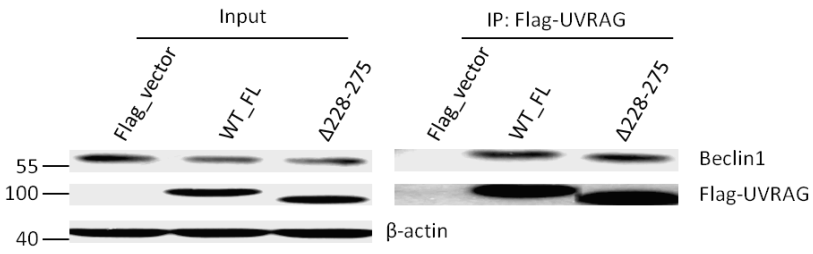

Figure 3. 2. 5 **Deletion mutation cannot abolish UVRAG-Beclin1 interaction.** HEK293T cells were transfected by Flag-vector, Flag-UVRAG or Flag-UVRAG deletion mutants. Twenty four hours after transfection, cell lysates were immunoprecipitated by anti-Flag magnetic beads and the immunocomplexes were analyzed by western blotting using anit-Beclin1 antibody.

While our initial co-ip data of the UVRAG mutants didn't agree with the *in vitro* ITC results in terms of their binding to Beclin1, multiple factors could have contributed to this discrepancy. First of all, the *in vitro* ITC experiments used only the coiled coil domain of Beclin1 and UVRAG, while the in vivo co-ip experiments used full-length proteins. Secondly co-ip assays are qualitative and sensitive assays that confirms co-precipitation but not necessarily direct physical interaction, while the in vitro ITC method provides quantitative measurement of direct physical interaction. Lastly there is also the possibility that other regions of Beclin1 or UVRAG may be involved in their interactions as well.

To further investigate the Beclin1-UVRAG interaction we generated a few deletion constructs for UVRAG. First we generated a UVRAG deletion mutant which has the Beclin1 interaction domain (228-275) truncated. Then we investigated the interaction between deletion mutant and Beclin1 by transfected HEK293T cells

with the Flag tagged UVRAG deletion mutant. Co-ip experiments were performed in the same manner as previous experimental settings. Interestingly, the deletion mutant could pull down considerable amount of Beclin1 (Fig 3.2.5). These data suggest that the Beclin1-interacting coiled coil region of UVRAG may not be exclusively responsible for the Beclin1-UVRAG interaction. It is possible other regions of UVRAG may interact with Beclin1 directly. There is also the other possibility that UVRAG can associate with third-party Beclin1-interacting proteins independent from its coiled coil domain.

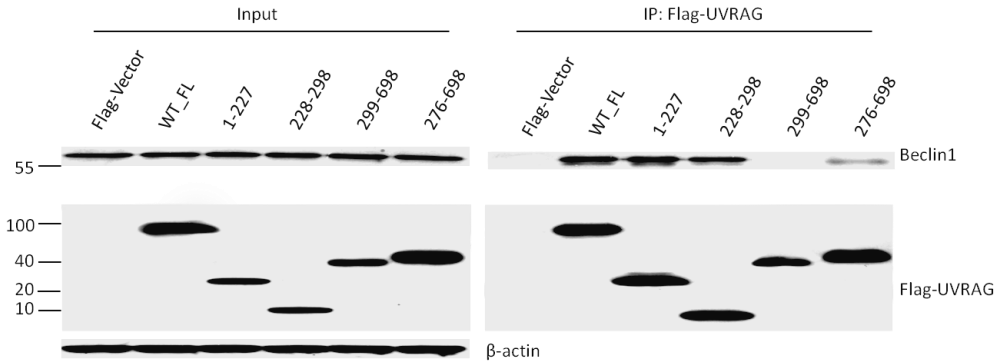

Figure 3. 2. 6 **Beclin1 interaction domain mapping.** HEK293T cells were transfected with a series of Flag-UVRAG deletion mutants. Twenty four hours after transfection, cell lysates were immunoprecipitated by anti-Flag magnetic beads and the immunocomplexes were analyzed by western blotting using anit-Beclin1 antibody.

To further analyze the Beclin1-interacting regions of UVRAG we decided to re-map the Beclin1 interaction domain on UVRAG. We generated a series of UVRAG truncation mutants to map the accurate boundary of Beclin1 interaction domain around 227-275 of UVRAG. And these truncated Flag-UVRAG constructs

were transfected to HEK293T and Co-ip assays were carried out as previous protocol to investigate their interactions with endogenous Beclin1. As shown in Fig 3.2.7, the constructs 1-227 and 228-298 pulled down comparable amount of Beclin1 to that of the full length UVRAG, and deletion of 1-275 significantly decreased the amount of Beclin1. Only the IP sample of 1-298 deleted construct showed undetectable Beclin1. These results show that Beclin1 interaction domain on UVRAG is located in the region of 1-298. Combined with previous reports (Liang et al., 2006) on the definition of UVRAG CCD domain, we generated several truncated mutants in the region before residue 298 and conducted the IP experiments in the same setup.

And we found that that only the deletion of the fragment from residue 199 to 298 of UVRAG could not pull down Beclin1 but the other constructs could. These results suggest that the short peptide fragment of 199-227 may contribute to Beclin1-UVRAG interaction, in addition to the coiled coil domain of 227-275. Currently there is no structural information on the 199-227 region. Whether and how this region affects the Beclin1-UVRAG interaction awaits further investigation.

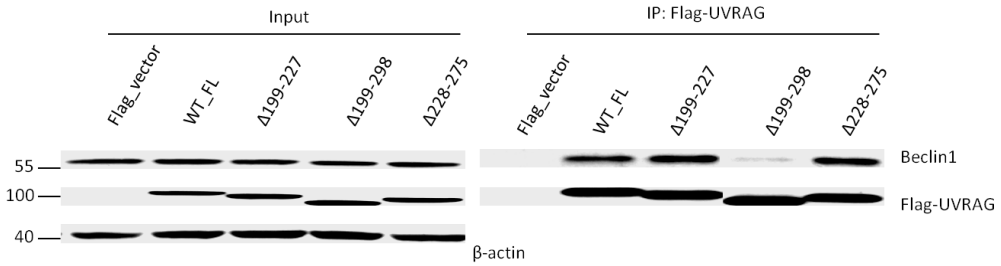

Figure 3. 2. 7 **Residue 199-298 of UVRAG is required for Beclin1 interaction.** HEK293T cells were transfected with a series of Flag-UVRAG deletion mutants. Twenty four hours after

transfection, cell lysates were immunoprecipitated by anti-Flag magnetic beads and the immunocomplexes were analyzed by western blotting using anit-Beclin1 antibody.

3.2.4 Mutations that perturb the Beclin1-UVRAG interaction favors the formation of Beclin1-Atg14L complex

Our previous data showed that UVRAG is a stronger binding partner than Atg14L for interaction with Beclin1 (Li et al., 2012). Moreover, it has been reported that both UVRAG and Atg14L bind to the same region of Beclin1, the CCD domain. We reason that the series of hydrophobic leucine zippers at the Beclin1-UVRAG interface might contribute to this stronger affinity. Furthermore we anticipate that the multi-site UVRAG mutants, with weakened or abolished binding to Beclin1, may lose their competitive advantage over Atg14L for binding to Beclin1. To testify our hypothesis, the UVRAG mutants which showed negative results in Beclin1 binding assays using ITC, were used *in vivo*. The UVRAG mutants and Atg14L wild type were co-transfected into HEK293T cells to investigate their interactions with Beclin1. And the IP experiments were performed by using anti-Flag beads and cell lysate from HEK293T cells transiently transfected with Flag-UVRAG mutants with or without over expression of Atg14L. Then, Beclin1 levels were detected in the IP complex.

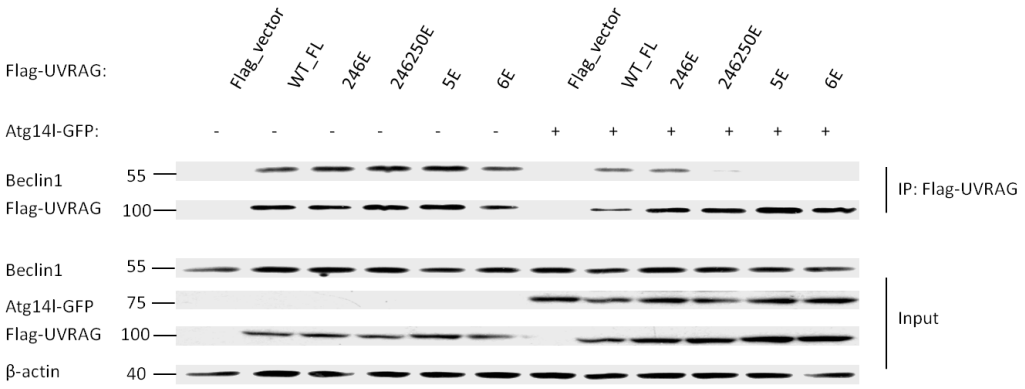

Figure 3. 2. 8 **Key residues on UVRAG are critical for competition with Atg14L.** HEK293 cells were transfected either with Flag-UVRAG mutants alone or together with GFP-Atg14L. Twenty four hours after transfection, cell lysates were immunoprecipitated by anti-Flag magnetic beads and the immunocomplexes were analyzed by western blotting using anit-Beclin1 antibody.

The competitive IP results show that all the mutants were able to intact with Beclin1 without significant differences when UVRAG mutants were transfected alone. However, when Atg14L were introduced into the cells, starting from the 246250E to the hexa mutants, the amount of Beclin1 pulled down by UVRAG decreased gradually and finally was totally absent for the hexa mutant (Fig 3.2.8). Inversely, the amount of Beclin1 pulled down by Atg14L increased for UVRAG mutants with more Leu→Glu mutation sites (Fig 3.2.9).

These data imply the essential roles of the leucine zipper between Beclin1 and UVRAG in the homeostasis of the Beclin1 containing complexes, especially in maintaining the balance between Atg14L-Beclin1 and UVRAG-Beclin1 complexes.

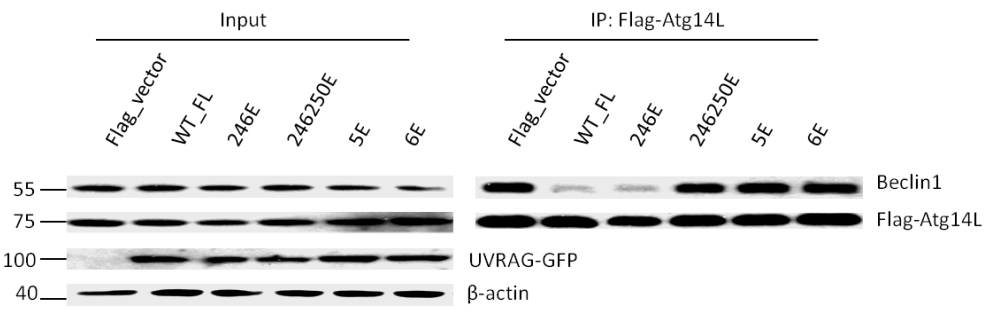

Figure 3. 2. 9 **Key residues on UVRAG prevent Beclin1-Atg14L binding.** HEK293T cells were transfected with GFP-UVRAG mutants and Flag-Atg14L plasmids. Twenty four hours after transfection, cell lysates were immunoprecipitated by anti-Flag magnetic beads and the immunocomplexes were analyzed by western blotting using anit-Beclin1 antibody.

3.2.5 The impact of UVRAG-Beclin1 interaction in autophagy

As the Co-IP data showed that the strong interaction between UVRAG and Becin1 played key roles in the dynamic balance in Beclin1 containing complexes, which had been reported to be essential for autophagy regulation, we next investigated the impact of overexpression of different UVRAG mutants on autophagy flux. HCT116 cells have been reported to contain a monoallelic deletion of UVRAG in the chromosome and have lower level of endogenous UVRAG compare to other cell lines (Ionov et al., 2004). Liang's group has also demonstrated that HCT116 has defect in autophagy and the exogenous expression of UVRAG can restore the autophagic flux in a Beclin1 dependent manner (Liang et al., 2006).

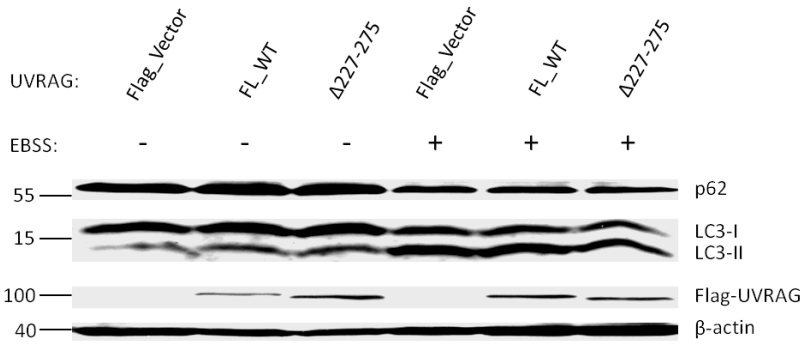

Figure 3. 2. 10 **Autophagy assay of overexpressed UVRAG mutants.** HCT116 cells were transfected by Flag-UVRAG mutants. Twenty four hours after transfection, cells were starved for 2hrs and the LC3 and p62 were visualized by western blotting using anti-LC3 and anti-p62.

Based on these reports, we transfected HCT116 cells with full length UVRAG or the truncation mutant (△227-275) to investigate whether Beclin1 interaction domain play a role in starvation induced autophagy. To do so, we monitored two well established autophagy markers, LC3-Ⅱ and p62, in the transiently UVRAG transfected HCT116 cells which has been starved in EBSS medium for two hours. However, no significant differences in the levels of LC3-II and p62 between full length and truncation mutant samples were observed during both normal condition and starvation. Furthermore, wild type UVRAG did not showed significant changes in the level of LC3-II and p62 compare to vector control. We also found that the turnover of p62 and conversion of LC3 in the vector control samples were quite obvious during starvation (Fig 3.2.10), which is inconsistent with previous report. The inconsistence may suggest the HCT116 cell line in our group is different from Liang's group, at least in the starvation induced starvation or there are some other

unknown reasons which need further investigations.

3.2.6 The Beclin1-UVRAG interaction is critical for endocytic pathway

UVRAG and Beclin1 have been reported to have essential functions in the endocytosis pathway which is particularly related to EGFR degradation. To find out whether the interaction between Beclin1 and UVRAG is involved in the regulation of endocytosis, HEK293T cells were transfected with wild type and UVRAG mutant plasmids and EGF treatment was performed 24hr after transfection. After EGF treatment as the indicated time, cells were collected and subjected to Western blotting to detect the amount of EGFR by anti-EGFR antibody.

In the Western Blot results, significant less EGFR were observed in wild type and 246E mutant of UVRAG from 30 minutes compare to vector control. The other mutants which lost the binding to Beclin1 *in vitro* showed the similar amount of EGFR as vector control at 30 minutes. And the EGFR bands nearly disappear at 50 minutes in wild type and single mutant group, but in double, penta and hexa mutant group, there is considerable amount of EGFR. The band of EGFR remains clearly in penta and hexa mutant even in 2 hours samples (Fig 3.2.11). These data indicates that the mutations on UVRAG which lead to loss of Beclin1 binding *in vitro* also lead to the loss of accelerative function in EGFR degradation. Furthermore, these data suggest that Beclin1-UVRAG interaction plays essential roles in EGFR degradation and endocytosis pathway. I have performed a series of experiments to assay EGFR

degradation and obtained preliminary data that is not shown here. The figure reported here is based on the experiments conducted by Wu Shuai, a graduate student in the lab. His results are included here to give a comprehensive report of the final data.

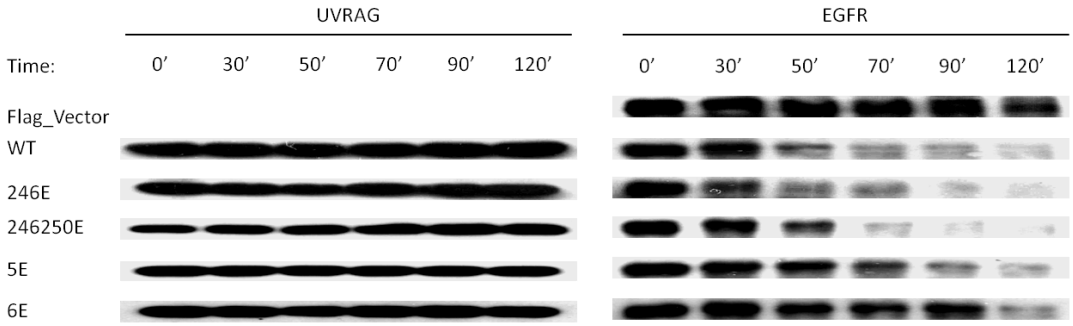

Figure 3. 2. 11 **EGFR degradation assay of overexpressed UVRAG mutants.** HEK293T cells were transfected either with empty vector or UVRAG mutants. Twenty four hours after transfection, cells were treated by 200ng/ml EGF for indicated time and EGFR amount were detected by western Blotting using anti-EGFR.

3.3 Structural and Functional Studies of the Beclin1-Vps34 Complex in Autophagy

Due to the complexity of the Vps34-Beclin1-containing complexes, the detailed physical interaction among the members of the complexes remains unclear. Our aim in this part is to conduct initial characterization of the interaction between Beclin1 and Vps34 through Co-ip and biochemical methods.

3.3.1 Mapping of Vps34 and Beclin1 interaction domains

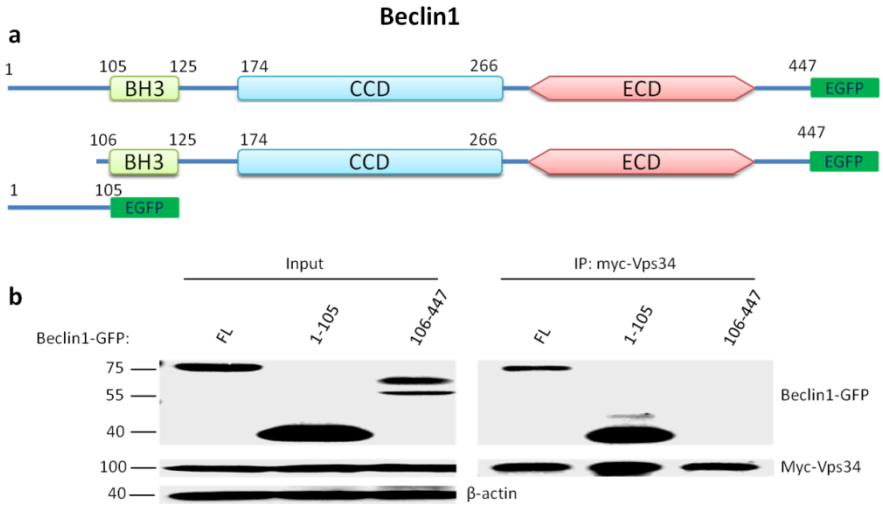

Figure 3. 3. 1 **N-terminal of Beclin1 is required for Vps34 binding.** a. the schematic picture of the Beclin1 constructs; b. Co-IP results, Beclin1-GFP constructs and myc-Vps34 were co-transfected into HEK293 cells, 24hrs after transfection IP was performed by anti-myc and results visualized by western blotting using anti-GFP.

The first thing we did is to determine the interaction domains on Beclin1 and Vps34. To identify the Vps34 interaction domain on Beclin1, a series of GFP tagged Beclin1 deletion mutants and myc tagged wild type Vps34 were constructed and

co-transfected into HEK293T cells. Twenty-four hours after transfection, the cells lysates were co-immunoprecipitated by anti-myc antibody. The IP complexes pulled down by myc-Vps34 were analyzed by Western Blot using anti-GFP. The Western Blot results show that the N-terminal region (Beclin1$^{1-105}$) can be pulled down by myc-Vps34, but the rest of Beclin1 without this region cannot (Fig 3.3.1). These data suggest that the N-terminal region (Beclin1$^{1-105}$) is required for binding to Vps34.

We employed similar strategy to search for the exact boundary of Beclin1 binding domain on Vps34. Briefly, we co-transfected a series of myc tagged Vps34 constructs and GFP tagged wild type Beclin1 into HEK293T cells. Twenty-four hours after transfection, the cells lysates were co-immunoprecipitated by anti-myc antibody. The IP complexes pulled down by myc-Vps34 were analyzed by Western Blot using anti-GFP. The results show that the construct C2T, with a 31 amino acid peptide from residue 214 to 244 truncated cannot pull down Beclin1, but C2S and wild type containing this fragment do. These data indicate that Vps34 fragment 214-244 is indispensable for the interaction with Beclin1.

Previous reports had revealed that Beclin1 plays key roles in the lipid kinase activity of Vps34. Next, we did is to investigate the kinase activity of the Vps34 construct which has lost the binding to Beclin1. We transfected myc tagged Vps34 wild type and deletion constructs C2T or C2S separately into HEK293 cells and conducted IP experiments using the protocol in domain mapping studies. Half of the IP complexes were subjected to kinase assays as described in materials and methods.

The kinase reaction products were analyzed by TLC and followed by autoradiography. The kinase assays results show that the IP complex from construct C2T has no endogenous Beclin1 and lose almost half of kinase activity compare to full length Vps34. Interestingly, the construct C2S which has residues 1-214 deleted also lost the interaction with endogenous Beclin1, and showed similar kinase activity to that of C2T (Fig 3.3.3). These data further confirm the essential roles of Beclin1 interaction for the kinase activity of Vps34 complex and the importance of Vps34 214-244 in binding to Beclin1. The performance of C2S suggests the region 1-214 also plays some roles in Beclin1 interaction or may be just caused by mis-fording originated from overexpression of truncated mutation. To clarify the performance of C2S, we need further investigations.

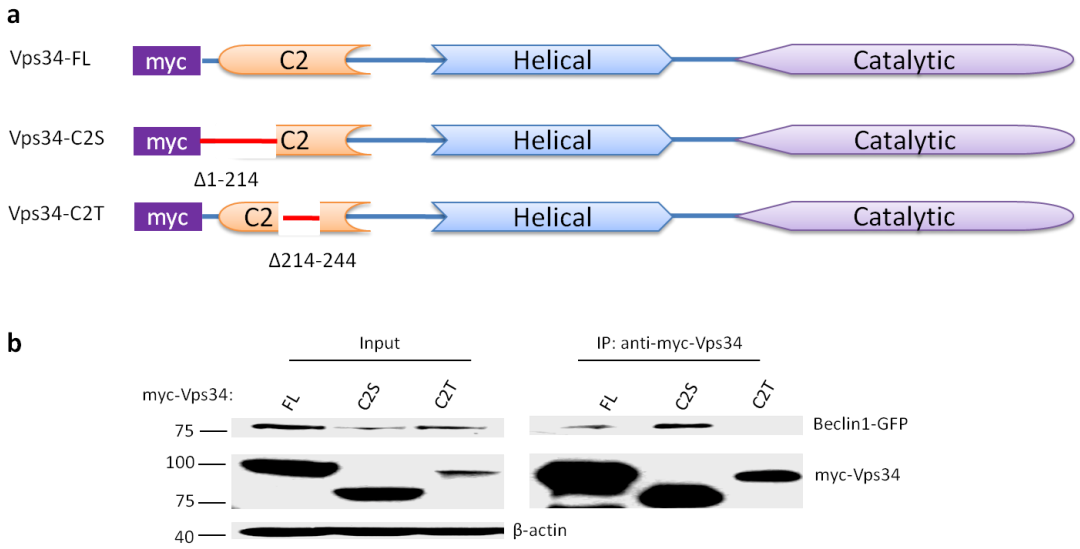

Figure 3. 3. 2 **Residue 214-244 (C2R) on Vps34 is required for Beclin1interaction.** a. the schematic picture of the Vps34 constructs; b. Co-IP results, myc-Vps34 deletion constructs and GFP-Beclin1 full length were co-transfected into HEK293 cells, 24hrs after transfection IP was performed by anti-myc

and results visualized by western blotting using anti-GFP.

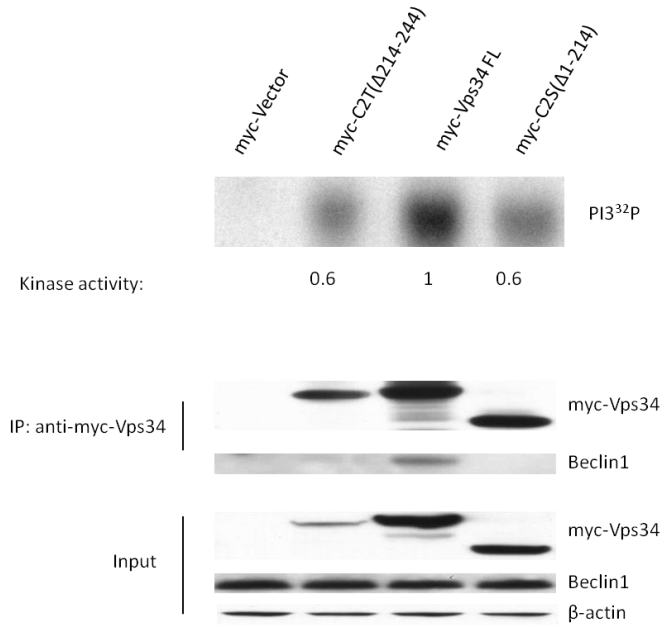

Figure 3. 3. 3 **C2R on Vps34 is required for Beclin1 binding and activity of the complex.** HEK293T cells were transfected with wild type or deletion mutated myc-Vps34, 24 hours later, cells were subjected to IP with anti-myc, and kinase activity assays were carried out with the purified IP complexes. The kinase activities were normalized by the amount of Vps34 in IP complexes.

3.3.2 Folding of the Vps34-Beclin1 interaction domains

Based on the domain mapping results which suggested that the fragment 1-244 in C2 domain of Vps34 is important for the binding of Beclin1, we generated a series of *E.coli* expression plasmids containing different fusion tag and various protein fragments of Vps34 C2 domain around residue 1-244 to search for soluble segments (Fig 3.3.4) and for further biochemical studies.

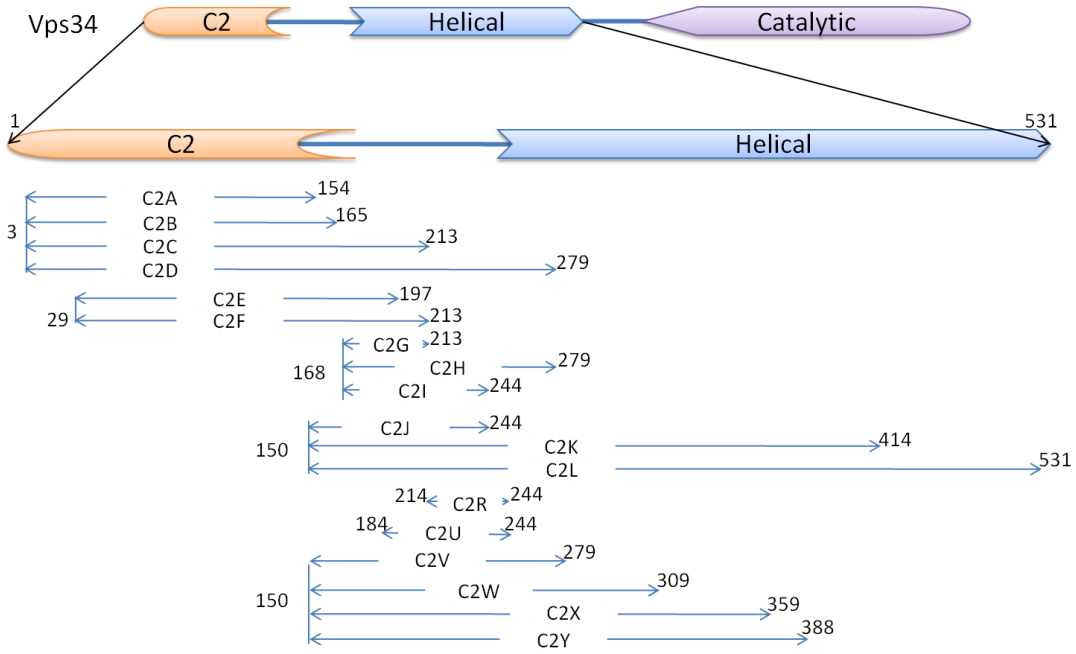

Figure 3. 3. 4 **Schematic picture of Vps34 C2 constructs for solubility screening.** The DNA sequence of the corresponding fragments were cloned to expression vectors and solubility of the fragments were tested in *E.coli.*

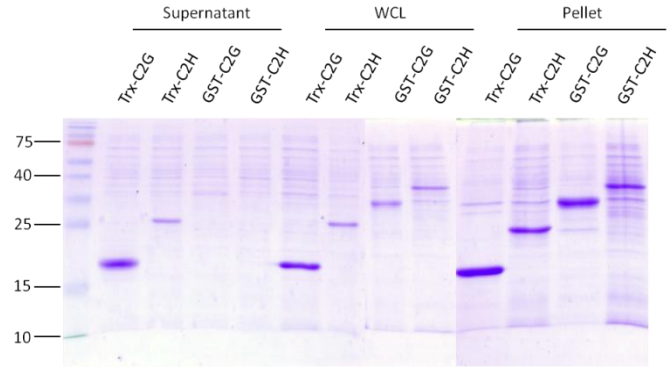

Figure 3. 3. 5 **Examples of solubility screening.** WCL: whole cell lysate

With IPTG induction, different constructs were overexpressed in *E.coli* BL-21(DE3) cells. Harvested cells were lysed by ultra-sonication in different buffers varying in pH from 3.5 to 10 and salt concentration from 50 to 1000mM. After

centrifugation, proper amount of whole cell lysis (WCL), pellets and supernatants were analyzed by SDS-PAGE with coomassie-blue staining. The results were evaluated by the intensity of corresponding bands in the supernatant fractions. For example, in the screening of C2G and C2H with Trx (thioredoxin) and GST (Glutathione S-transferases) fusion tag using His-binding buffer (20mM sodium phosphate, pH7.4, 500mM NaCl, 40mM imidazole) as lysis buffer, the solubility of Trx-C2G was considered as "++", and Trx-C2H and GST-C2G as "+", while GST-C2H as "-" (Fig 3.3.5). The solubility screening results were summarized in Table 3.3.1.

Fragments	Solubility of fragments with different fusion tag			
	pET32M (Trx)	pET49M (GST)	pETM (6Xhis)	pMBP (MBP)
C2A	-	-	--------	**+**
C2B	-	-	--------	-
C2C	-	-	--------	-
C2D	-	-	--------	-
C2E	-	-	--------	**++**
C2F	-	-	--------	-
C2G	**++**	**+**	--------	--------
C2H	**+**	-	--------	--------
C2I	-	--------	--------	--------
C2J	**++**	--------	**+**	--------
C2K	-	--------	--------	--------
C2L	-	--------	--------	--------
C2R	**++**	-	-	--------
C2U	--------	--------	-	--------
C2V	--------	--------	-	--------
C2W	--------	--------	-	--------
C2X	--------	--------	-	--------
C2Y	--------	--------	-	--------

Table 3. 3. 1 **Summary of solubility screening of the Vps34 C2 domain.** Note: "++" means good

solubility; "+" means soluble; "_" means poor solubility and not suitable for purification; "--------" means construct has not been tried in this vector.

As shown in Table 3.3.1, constructs MBP-C2A, MBP-C2E, Trx - and GST-C2G, Trx-C2H, Trx- and 6*His- C2J and Trx-C2R were selected to proceed to purification. Except C2J and C2G, all the constructs had aggregation problem during the purification steps, especially in the fusion tag removing step. The construct C2J could be prepared by affinity and size-exclusion chromatography as depicted in Methods and Material.

Then we studied the folding state of Vps34 C2J by NMR. The C2J proteins prepare from normal LB broth were resolved in PBS with 10% DO_2 in a concentration of 0.5mM for NMR tests. Judged by the 1D NMR spectra, C2J showed obvious unfolded random coil characteristics (Fig 3.3.6).

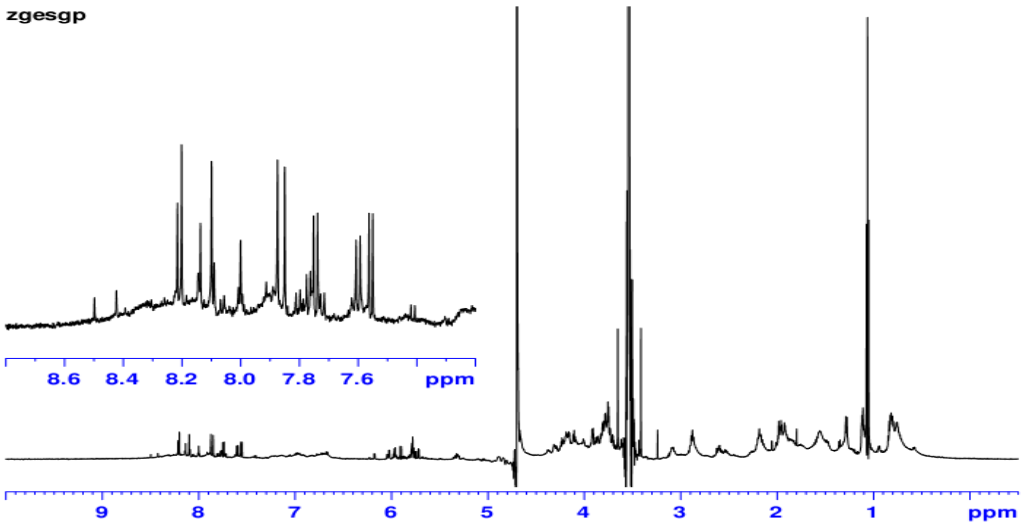

Figure 3. 3. 6 **^{1}H-NMR spectra of Vps34 C2J.** The NMR profile was collected using native C2J with 10%

DO_2. The signals from 7.2 to 8.8 ppm were enlarged on the up-left panel.

In order to resolve the folding problem, we co-expressed the proposed binding partner for Vps34 C2J, N-terminal of Beclin1, to help it transform to a folded state for further biochemical and structural studies.

3.3.3 Folding of Beclin1-Vps34 linked constructs

A 5X(GS) linker was used to conjugate the proposed binding partners, C2J of Vps34 and Beclin11-105, to overexpress them in *E.coli* (Fig 3.3.7) aimed to facilitate their folding.

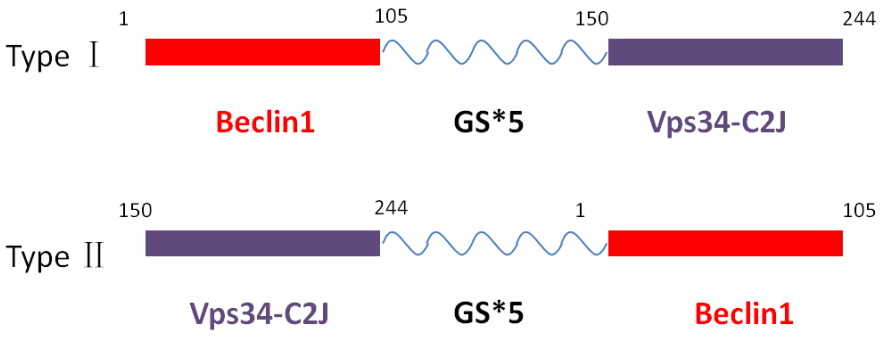

Figure 3. 3. 7 **Schematic pictures of two types of linked constructs.**

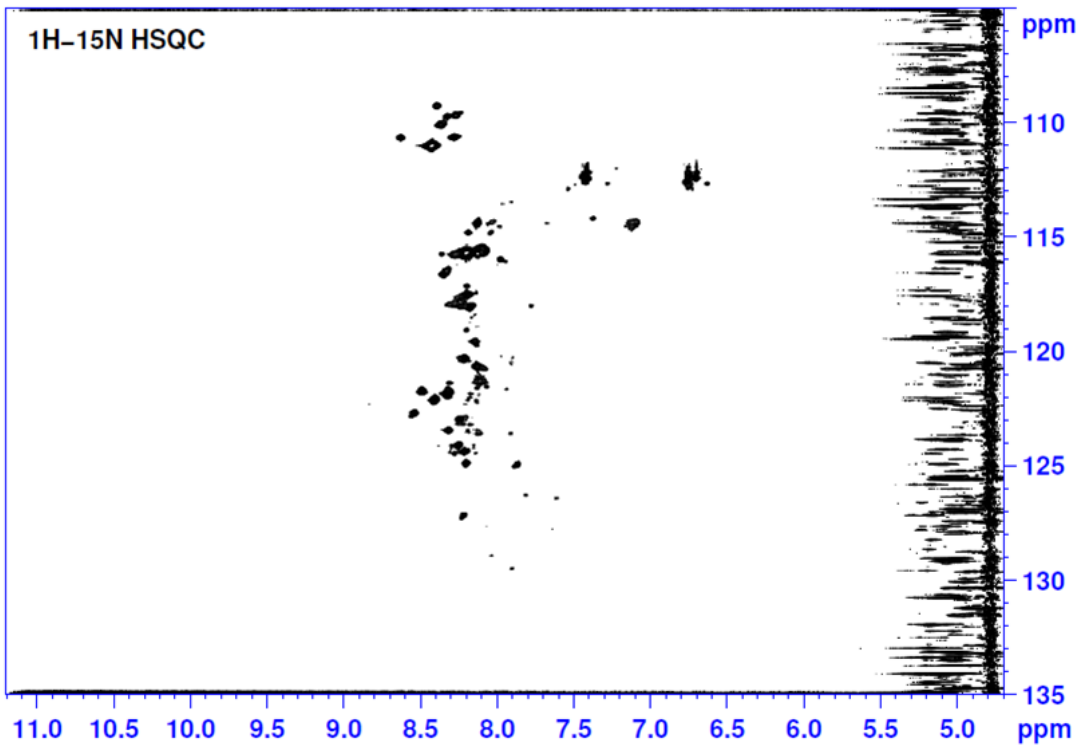

Figure 3. 3. 8 **^{1}H-^{15}N HSQC spectra of ^{15}N-labeled Vps34_C2J-(GS)*5-Beclin1_1-105**. NMR spectra was obtained by ^{15}N-labeled Vps34_C2J-(GS)*5-Beclin1_1-105 with 10% DO_2.

Interestingly, the type I construct with Beclin1 1-105 in the N-terminal of the aggregated during concentration; while the type II construct which with Vps34 C2J in the N-terminal could proceed to purification. To study the folding state of the complex, 2D NMR was performed using ^{15}N labeled type II construct Vps34_C2J-(GS)*5-Beclin1_1-105 prepared in M9 medium. However, in the 2D NMR spectra, all the cross-peaks from main chain amide groups were stacked in a small region, indicating an unfolded state (Fig3.3.8).

Chapter4 Discussions and Summary

4.1 P62 S409 phosphorylation promotes p62-ubiquitin interaction

In this part, we quantified the binding affinities to ubiquitin of p62 UBA wild type, S409A mutant and S409E mutant. Consistent with our collaborator's data, our S409E mutant, which mimics the phosphorylation of S409 in p62, leads to increased interaction with ubiquitinated proteins. We found that by ITC measurements S409E showed stronger affinity to ubiquitin than wild type, while S409A mutant that mimicks phosphorylation deficiency shows the lowest affinity to ubiquitin. Furthermore our DSC measurements show reduced thermal stability of S409E as compared to wild-type, suggesting decreased structural stability.

The crystal structure of p62 UBA domain adopts a dimeric form in one crystallographic asymmetric unit. Consistently, analytical gel-filtration and ultracentrifugation indicate that UBA domain exists as a dimer in solution (Isogai et al., 2011). S409 is located quite close to the dimerization interface that consists of F408, W414 and L418. And it has been reported that the monomer derivatives of GST fused p62 UBA domain bind more strongly to tetra-ubiquitins than wild type (Isogai et al., 2011). We propose that p62 S409 phosphorylation might disturb the dimerization of UBA domain to enhance its ubiquitin binding affinity.

4.2 Beclin1-UVRAG complex in autophagy and endosomal trafficking

The crystal structure of Beclin1-UVRAG complex reveals a parallel coiled coil assembly with five leucine zipper pairs at the interface. These leucine zippers, together with electrostatic interactions, render the Beclin1-UVRAG interaction highly stable. Through site-directed mutagenesis, we confirmed that multi-site mutations that replace a series of hydrophobic leucine residues with charged glutamate is necessary to significantly weaken or abolish the Beclin1-UVRAG interaction. Furthermore UVRAG mutations that weaken the Beclin1-UVRAG interaction would favor the formation of the Beclin1-Atg14L complex at the expense of the Beclin1-UVRAG complex, further comfirming the mutual exclusivity of these two complexes.

Our extensive effort to characterize the impact of UVRAG mutations on autophay yielded little results. Our data show that the HCC116 (???) cell line we used, which supposedly carries monoallelic loss of UVRAG and should have impaired autophagy, have instead normal level of autophagy activity upon starvation. Furthermore over-expressing the various UVRAG mutants in this cell line shows little impact on its autophay activity. While our data is not information we should bear in mind that our experiments were carried out with serious limiting factors. There are many ways to improve our experiments, such as generating UVRAG knockdown cell lines, and stably over-expressing UVRAG mutants etc. These

experiments should be our future studies.

In contrast to the findings of Zeng et al. and Liang et al., Harald Stenmark' group showed significant down regulation of EGFR degradation by Beclin1 knock down (Liang et al., 2006; Thoresen et al., 2010; Zeng et al., 2006). They also demonstrated that knock down of Vps15, Vps34, UVRAG and Bif-1 strongly suppressed the endocytosis pathway. All these data suggest a complex composed of Bif-1-UVRAG-Beclin1-Vps34-Vps15 is the regulation machinery in the endocytosis pathway. We detected the EGFR degradation in HEK293T cells with transient overexpression of different UVRAG mutants. And we found that the mutants that lost the binding to Beclin1 *in vitro* showed declined ability in promoting the degradation of EGFR compare to wild type UVRAG. Our findings confirm the roles of UVRAG in the endocytosis pathway.

4.3 Preliminary studies of Beclin1-Vps34 interaction

In this part, we identified a fragment from residue 214 to 244 in the C2 domain of Vps34 as the Beclin1 binding region. Also, we found that the overexpressed N-terminal of Beclin1 (1-105) was sufficient for the interaction with Vps34 in HEK293 cells. Based on that, we overexpressed Beclin1 $^{1\text{-}105}$ and Vps34 $^{214\text{-}244}$ in *E.coli* independently, but encountered with aggregation problem during the purification. Through solubility screening with a series of constructs of Vps34 C2 domain, C2J is found to be good enough for purification. However, C2J showed typical unfolding characteristics during gel filtration and 1D NMR assays. To resolve the folding problem, we used a 5X(GS) linker to conjugate the Beclin1 $^{1\text{-}105}$ and Vps34 $^{150\text{-}244}$ (C2J) and expressed them as a single molecule in *E.coli* cells. This strategy largely improved the solubility and resolved the aggregation problems in purification. The folding state of ^{15}N-labeled linked complex was studied by ^{1}H-^{15}N HSQC. Unfortunately, the HSQC spectra still showed the characteristics of unfolding proteins.

Meanwhile, we investigated the *in vitro* kinase activities of the Vps34 complexes containing wild type Vps34 and the Becin1-binding-deficient mutants. The deletion of the Beclin1 binding region on Vps34 strikingly decreased the kinase activity of the IP complex. These data suggest that Beclin1 is strongly required for Vps34 complex kinase activity.

During the domain mapping, we found some conflicts with previous report.

Beclin1 ECD+CCD domain was reported to be the binding region of Vps34, but we found that the N-terminal region was sufficient for the interaction and showed much stronger affinity to Vps34 than that of the rest part of Beclin1. The failure to get a well folded linked complex composed of Beclin1 $^{1\text{-}105}$ and Vps34 $^{150\text{-}244}$ made it hard to identify the physical interaction between them. However, there is also no solid evidence for the direct interaction between Vps34 and the Beclin1$^{106\text{-}447}$ till now. These conflicts raise a concern on using IP experiments to identify the interaction domains of Beclin1 and Vps34. And also the overexpression of truncated or fragmented proteins may cause abnormal folding and sequential false positive or negative results. In the other side, these data may also imply the architectural complexity of the Beclin1-Vps34 complex.

This part of work obviously needs further investigation in the future. We will continue studies in following aspects: 1) Continue mapping the Vps34 interaction domain on Beclin1 by Co-IP with overexpression of Beclin1 constructs alone; 2) Use co-expression vectors in *E.coli* system to find the Vps34 C2J binding partner; 3) Use mammalian expression systems to obtain larger complexes containing other components in the complex, such as Atg14 and Vps15.

References

Amaravadi, R.K., Yu, D., Lum, J.J., Bui, T., Christophorou, M.A., Evan, G.I., Thomas-Tikhonenko, A., and Thompson, C.B. (2007). Autophagy inhibition enhances therapy-induced apoptosis in a Myc-induced model of lymphoma. J Clin Invest *117*, 326-336.

Arndt, V., Dick, N., Tawo, R., Dreiseidler, M., Wenzel, D., Hesse, M., Furst, D.O., Saftig, P., Saint, R., Fleischmann, B.K., *et al.* (2010). Chaperone-assisted selective autophagy is essential for muscle maintenance. Curr Biol *20*, 143-148.

Axe, E.L., Walker, S.A., Manifava, M., Chandra, P., Roderick, H.L., Habermann, A., Griffiths, G., and Ktistakis, N.T. (2008). Autophagosome formation from membrane compartments enriched in phosphatidylinositol 3-phosphate and dynamically connected to the endoplasmic reticulum. J Cell Biol *182*, 685-701.

Bechtel, W., Helmstadter, M., Balica, J., Hartleben, B., Kiefer, B., Hrnjic, F., Schell, C., Kretz, O., Liu, S., Geist, F., *et al.* (2013). Vps34 deficiency reveals the importance of endocytosis for podocyte homeostasis. J Am Soc Nephrol *24*, 727-743.

Bergamini, E. (2005). Targets for antiageing drugs. Expert Opin Ther Targets *9*, 77-82.

Bernales, S., McDonald, K.L., and Walter, P. (2006). Autophagy counterbalances endoplasmic reticulum expansion during the unfolded protein response. PLoS Biol *4*, e423.

Boya, P., Reggiori, F., and Codogno, P. (2013). Emerging regulation and functions of

autophagy. Nat Cell Biol *15*, 713-720.

Cavey, J.R., Ralston, S.H., Hocking, L.J., Sheppard, P.W., Ciani, B., Searle, M.S., and Layfield, R. (2005). Loss of ubiquitin-binding associated with Paget's disease of bone p62 (SQSTM1) mutations. J Bone Miner Res *20*, 619-624.

Cecconi, F., and Levine, B. (2008). The role of autophagy in mammalian development: cell makeover rather than cell death. Dev Cell *15*, 344-357.

Cheng, H.C., Kim, S.R., Oo, T.F., Kareva, T., Yarygina, O., Rzhetskaya, M., Wang, C., During, M., Talloczy, Z., Tanaka, K., *et al.* (2011). Akt suppresses retrograde degeneration of dopaminergic axons by inhibition of macroautophagy. J Neurosci *31*, 2125-2135.

De Duve, C., and Wattiaux, R. (1966). Functions of lysosomes. Annu Rev Physiol *28*, 435-492.

Del Roso, A., Vittorini, S., Cavallini, G., Donati, A., Gori, Z., Masini, M., Pollera, M., and Bergamini, E. (2003). Ageing-related changes in the in vivo function of rat liver macroautophagy and proteolysis. Exp Gerontol *38*, 519-527.

Deretic, V. (2009). Multiple regulatory and effector roles of autophagy in immunity. Curr Opin Immunol *21*, 53-62.

Deretic, V. (2011). Autophagy in immunity and cell-autonomous defense against intracellular microbes. Immunol Rev *240*, 92-104.

Di Bartolomeo, S., Corazzari, M., Nazio, F., Oliverio, S., Lisi, G., Antonioli, M., Pagliarini, V., Matteoni, S., Fuoco, C., Giunta, L., *et al.* (2010). The dynamic interaction of AMBRA1 with the dynein motor complex regulates mammalian

autophagy. J Cell Biol *191*, 155-168.

Ding, Z.B., Hui, B., Shi, Y.H., Zhou, J., Peng, Y.F., Gu, C.Y., Yang, H., Shi, G.M., Ke, A.W., Wang, X.Y., *et al.* (2011). Autophagy activation in hepatocellular carcinoma contributes to the tolerance of oxaliplatin via reactive oxygen species modulation. Clin Cancer Res *17*, 6229-6238.

Donati, A., Cavallini, G., Paradiso, C., Vittorini, S., Pollera, M., Gori, Z., and Bergamini, E. (2001). Age-related changes in the regulation of autophagic proteolysis in rat isolated hepatocytes. J Gerontol A Biol Sci Med Sci *56*, B288-293.

Duran, A., Linares, J.F., Galvez, A.S., Wikenheiser, K., Flores, J.M., Diaz-Meco, M.T., and Moscat, J. (2008). The signaling adaptor p62 is an important NF-kappaB mediator in tumorigenesis. Cancer Cell *13*, 343-354.

Efeyan, A., and Sabatini, D.M. (2010). mTOR and cancer: many loops in one pathway. Curr Opin Cell Biol *22*, 169-176.

Eisenberg-Lerner, A., and Kimchi, A. (2012). PKD is a kinase of Vps34 that mediates ROS-induced autophagy downstream of DAPk. Cell Death Differ *19*, 788-797.

Eisenberg, T., Knauer, H., Schauer, A., Buttner, S., Ruckenstuhl, C., Carmona-Gutierrez, D., Ring, J., Schroeder, S., Magnes, C., Antonacci, L., *et al.* (2009). Induction of autophagy by spermidine promotes longevity. Nat Cell Biol *11*, 1305-1314.

Esclatine, A., Chaumorcel, M., and Codogno, P. (2009). Macroautophagy signaling

and regulation. Curr Top Microbiol Immunol *335*, 33-70.

Farre, J.C., Krick, R., Subramani, S., and Thumm, M. (2009). Turnover of organelles by autophagy in yeast. Curr Opin Cell Biol *21*, 522-530.

Fimia, G.M., Stoykova, A., Romagnoli, A., Giunta, L., Di Bartolomeo, S., Nardacci, R., Corazzari, M., Fuoco, C., Ucar, A., Schwartz, P., *et al.* (2007). Ambra1 regulates autophagy and development of the nervous system. Nature *447*, 1121-1125.

Funderburk, S.F., Wang, Q.J., and Yue, Z. (2010). The Beclin 1-VPS34 complex--at the crossroads of autophagy and beyond. Trends Cell Biol *20*, 355-362.

Fung, C., Lock, R., Gao, S., Salas, E., and Debnath, J. (2008). Induction of autophagy during extracellular matrix detachment promotes cell survival. Mol Biol Cell *19*, 797-806.

Furuya, T., Kim, M., Lipinski, M., Li, J., Kim, D., Lu, T., Shen, Y., Rameh, L., Yankner, B., Tsai, L.H., *et al.* (2010). Negative regulation of Vps34 by Cdk mediated phosphorylation. Mol Cell *38*, 500-511.

Germain, M., Nguyen, A.P., Le Grand, J.N., Arbour, N., Vanderluit, J.L., Park, D.S., Opferman, J.T., and Slack, R.S. (2011). MCL-1 is a stress sensor that regulates autophagy in a developmentally regulated manner. EMBO J *30*, 395-407.

Gewirtz, D.A. (2014). The four faces of autophagy: implications for cancer therapy. Cancer Res *74*, 647-651.

Giordano, S., Darley-Usmar, V., and Zhang, J. (2014). Autophagy as an essential cellular antioxidant pathway in neurodegenerative disease. Redox Biol *2*, 82-90.

Goldman, S.J., Taylor, R., Zhang, Y., and Jin, S. (2010). Autophagy and the degradation of mitochondria. Mitochondrion *10*, 309-315.

Guo, J.Y., Chen, H.Y., Mathew, R., Fan, J., Strohecker, A.M., Karsli-Uzunbas, G., Kamphorst, J.J., Chen, G., Lemons, J.M., Karantza, V., *et al.* (2011). Activated Ras requires autophagy to maintain oxidative metabolism and tumorigenesis. Genes Dev *25*, 460-470.

Gurkar, A.U., Chu, K., Raj, L., Bouley, R., Lee, S.H., Kim, Y.B., Dunn, S.E., Mandinova, A., and Lee, S.W. (2013). Identification of ROCK1 kinase as a critical regulator of Beclin1-mediated autophagy during metabolic stress. Nat Commun *4*, 2189.

Gurusamy, N., Lekli, I., Gorbunov, N.V., Gherghiceanu, M., Popescu, L.M., and Das, D.K. (2009). Cardioprotection by adaptation to ischaemia augments autophagy in association with BAG-1 protein. J Cell Mol Med *13*, 373-387.

Hamacher-Brady, A., Brady, N.R., and Gottlieb, R.A. (2006). Enhancing macroautophagy protects against ischemia/reperfusion injury in cardiac myocytes. J Biol Chem *281*, 29776-29787.

Hamasaki, M., Noda, T., Baba, M., and Ohsumi, Y. (2005). Starvation triggers the delivery of the endoplasmic reticulum to the vacuole via autophagy in yeast. Traffic *6*, 56-65.

Hara, T., Nakamura, K., Matsui, M., Yamamoto, A., Nakahara, Y., Suzuki-Migishima, R., Yokoyama, M., Mishima, K., Saito, I., Okano, H., *et al.* (2006). Suppression of basal autophagy in neural cells causes neurodegenerative disease in mice.

Nature *441*, 885-889.

He, C., and Levine, B. (2010). The Beclin 1 interactome. Curr Opin Cell Biol *22*, 140-149.

He, S., Ni, D., Ma, B., Lee, J.H., Zhang, T., Ghozalli, I., Pirooz, S.D., Zhao, Z., Bharatham, N., Li, B., *et al.* (2013). PtdIns(3)P-bound UVRAG coordinates Golgi-ER retrograde and Atg9 transport by differential interactions with the ER tether and the beclin 1 complex. Nat Cell Biol *15*, 1206-1219.

Huang, C., Andres, A.M., Ratliff, E.P., Hernandez, G., Lee, P., and Gottlieb, R.A. (2011). Preconditioning involves selective mitophagy mediated by Parkin and p62/SQSTM1. PLoS One *6*, e20975.

Huang, C., Yitzhaki, S., Perry, C.N., Liu, W., Giricz, Z., Mentzer, R.M., Jr., and Gottlieb, R.A. (2010). Autophagy induced by ischemic preconditioning is essential for cardioprotection. J Cardiovasc Transl Res *3*, 365-373.

Hubbard, V.M., Valdor, R., Patel, B., Singh, R., Cuervo, A.M., and Macian, F. (2010). Macroautophagy regulates energy metabolism during effector T cell activation. J Immunol *185*, 7349-7357.

Ionov, Y., Nowak, N., Perucho, M., Markowitz, S., and Cowell, J.K. (2004). Manipulation of nonsense mediated decay identifies gene mutations in colon cancer Cells with microsatellite instability. Oncogene *23*, 639-645.

Ishii, T., Yanagawa, T., Kawane, T., Yuki, K., Seita, J., Yoshida, H., and Bannai, S. (1996). Murine peritoneal macrophages induce a novel 60-kDa protein with structural similarity to a tyrosine kinase p56lck-associated protein in response to

oxidative stress. Biochem Biophys Res Commun *226*, 456-460.

Isogai, S., Morimoto, D., Arita, K., Unzai, S., Tenno, T., Hasegawa, J., Sou, Y.S., Komatsu, M., Tanaka, K., Shirakawa, M., *et al.* (2011). Crystal structure of the ubiquitin-associated (UBA) domain of p62 and its interaction with ubiquitin. J Biol Chem *286*, 31864-31874.

Itakura, E., Kishi, C., Inoue, K., and Mizushima, N. (2008). Beclin 1 forms two distinct phosphatidylinositol 3-kinase complexes with mammalian Atg14 and UVRAG. Mol Biol Cell *19*, 5360-5372.

Itakura, E., and Mizushima, N. (2010). Characterization of autophagosome formation site by a hierarchical analysis of mammalian Atg proteins. Autophagy *6*, 764-776.

Jaber, N., Dou, Z., Chen, J.S., Catanzaro, J., Jiang, Y.P., Ballou, L.M., Selinger, E., Ouyang, X., Lin, R.Z., Zhang, J., *et al.* (2012). Class III PI3K Vps34 plays an essential role in autophagy and in heart and liver function. Proc Natl Acad Sci U S A *109*, 2003-2008.

Jahreiss, L., Menzies, F.M., and Rubinsztein, D.C. (2008). The itinerary of autophagosomes: from peripheral formation to kiss-and-run fusion with lysosomes. Traffic *9*, 574-587.

Jain, A., Lamark, T., Sjottem, E., Larsen, K.B., Awuh, J.A., Overvatn, A., McMahon, M., Hayes, J.D., and Johansen, T. (2010). p62/SQSTM1 is a target gene for transcription factor NRF2 and creates a positive feedback loop by inducing antioxidant response element-driven gene transcription. J Biol Chem *285*,

22576-22591.

Jia, K., Hart, A.C., and Levine, B. (2007). Autophagy genes protect against disease caused by polyglutamine expansion proteins in Caenorhabditis elegans. Autophagy *3*, 21-25.

Jin, Z., Li, Y., Pitti, R., Lawrence, D., Pham, V.C., Lill, J.R., and Ashkenazi, A. (2009). Cullin3-based polyubiquitination and p62-dependent aggregation of caspase-8 mediate extrinsic apoptosis signaling. Cell *137*, 721-735.

Jounai, N., Kobiyama, K., Shiina, M., Ogata, K., Ishii, K.J., and Takeshita, F. (2011). NLRP4 negatively regulates autophagic processes through an association with beclin1. J Immunol *186*, 1646-1655.

Joung, I., Strominger, J.L., and Shin, J. (1996). Molecular cloning of a phosphotyrosine-independent ligand of the p56lck SH2 domain. Proc Natl Acad Sci U S A *93*, 5991-5995.

Juhasz, G., Erdi, B., Sass, M., and Neufeld, T.P. (2007). Atg7-dependent autophagy promotes neuronal health, stress tolerance, and longevity but is dispensable for metamorphosis in Drosophila. Genes Dev *21*, 3061-3066.

Kabeya, Y., Mizushima, N., Yamamoto, A., Oshitani-Okamoto, S., Ohsumi, Y., and Yoshimori, T. (2004). LC3, GABARAP and GATE16 localize to autophagosomal membrane depending on form-II formation. J Cell Sci *117*, 2805-2812.

Kang, R., Zeh, H.J., Lotze, M.T., and Tang, D. (2011). The Beclin 1 network regulates autophagy and apoptosis. Cell Death Differ *18*, 571-580.

Kanki, T., Wang, K., Baba, M., Bartholomew, C.R., Lynch-Day, M.A., Du, Z., Geng, J., Mao, K., Yang, Z., Yen, W.L., *et al.* (2009). A genomic screen for yeast mutants defective in selective mitochondria autophagy. Mol Biol Cell *20*, 4730-4738.

Kaushik, S., Bandyopadhyay, U., Sridhar, S., Kiffin, R., Martinez-Vicente, M., Kon, M., Orenstein, S.J., Wong, E., and Cuervo, A.M. (2011). Chaperone-mediated autophagy at a glance. J Cell Sci *124*, 495-499.

Kim, J., Kim, Y.C., Fang, C., Russell, R.C., Kim, J.H., Fan, W., Liu, R., Zhong, Q., and Guan, K.L. (2013). Differential regulation of distinct Vps34 complexes by AMPK in nutrient stress and autophagy. Cell *152*, 290-303.

Kim, P.K., Hailey, D.W., Mullen, R.T., and Lippincott-Schwartz, J. (2008). Ubiquitin signals autophagic degradation of cytosolic proteins and peroxisomes. Proc Natl Acad Sci U S A *105*, 20567-20574.

Kirisako, T., Baba, M., Ishihara, N., Miyazawa, K., Ohsumi, M., Yoshimori, T., Noda, T., and Ohsumi, Y. (1999). Formation process of autophagosome is traced with Apg8/Aut7p in yeast. J Cell Biol *147*, 435-446.

Klionsky, D.J. (2005a). Autophagy. Curr Biol *15*, R282-283.

Klionsky, D.J. (2005b). The molecular machinery of autophagy: unanswered questions. J Cell Sci *118*, 7-18.

Klionsky, D.J. (2007). Autophagy: from phenomenology to molecular understanding in less than a decade. Nat Rev Mol Cell Biol *8*, 931-937.

Klionsky, D.J., and Emr, S.D. (2000). Autophagy as a regulated pathway of cellular

degradation. Science *290*, 1717-1721.

Knaevelsrud, H., Ahlquist, T., Merok, M.A., Nesbakken, A., Stenmark, H., Lothe, R.A., and Simonsen, A. (2010). UVRAG mutations associated with microsatellite unstable colon cancer do not affect autophagy. Autophagy *6*, 863-870.

Komatsu, M., Waguri, S., Chiba, T., Murata, S., Iwata, J., Tanida, I., Ueno, T., Koike, M., Uchiyama, Y., Kominami, E., *et al.* (2006). Loss of autophagy in the central nervous system causes neurodegeneration in mice. Nature *441*, 880-884.

Koneri, K., Goi, T., Hirono, Y., Katayama, K., and Yamaguchi, A. (2007). Beclin 1 gene inhibits tumor growth in colon cancer cell lines. Anticancer Res *27*, 1453-1457.

Kraft, C., Deplazes, A., Sohrmann, M., and Peter, M. (2008). Mature ribosomes are selectively degraded upon starvation by an autophagy pathway requiring the Ubp3p/Bre5p ubiquitin protease. Nat Cell Biol *10*, 602-610.

Kuma, A., and Mizushima, N. (2010). Physiological role of autophagy as an intracellular recycling system: with an emphasis on nutrient metabolism. Semin Cell Dev Biol *21*, 683-690.

Kuma, A., Mizushima, N., Ishihara, N., and Ohsumi, Y. (2002). Formation of the approximately 350-kDa Apg12-Apg5.Apg16 multimeric complex, mediated by Apg16 oligomerization, is essential for autophagy in yeast. J Biol Chem *277*, 18619-18625.

Lacoste-Collin, L., Garcia, V., Uro-Coste, E., Arne-Bes, M.C., Durand, D., Levade,

T., and Delisle, M.B. (2002). Danon's disease (X-linked vacuolar cardiomyopathy and myopathy): a case with a novel Lamp-2 gene mutation. Neuromuscul Disord *12*, 882-885.

Lamark, T., Kirkin, V., Dikic, I., and Johansen, T. (2009). NBR1 and p62 as cargo receptors for selective autophagy of ubiquitinated targets. Cell Cycle *8*, 1986-1990.

Laurin, N., Brown, J.P., Morissette, J., and Raymond, V. (2002). Recurrent mutation of the gene encoding sequestosome 1 (SQSTM1/p62) in Paget disease of bone. Am J Hum Genet *70*, 1582-1588.

Lee, H.K., Mattei, L.M., Steinberg, B.E., Alberts, P., Lee, Y.H., Chervonsky, A., Mizushima, N., Grinstein, S., and Iwasaki, A. (2010). In vivo requirement for Atg5 in antigen presentation by dendritic cells. Immunity *32*, 227-239.

Levine, B., and Kroemer, G. (2008). Autophagy in the pathogenesis of disease. Cell *132*, 27-42.

Li, J., Hou, N., Faried, A., Tsutsumi, S., and Kuwano, H. (2010). Inhibition of autophagy augments 5-fluorouracil chemotherapy in human colon cancer in vitro and in vivo model. Eur J Cancer *46*, 1900-1909.

Li, X., He, L., Che, K.H., Funderburk, S.F., Pan, L., Pan, N., Zhang, M., Yue, Z., and Zhao, Y. (2012). Imperfect interface of Beclin1 coiled-coil domain regulates homodimer and heterodimer formation with Atg14L and UVRAG. Nat Commun *3*, 662.

Liang, C., E, X., and Jung, J.U. (2008a). Downregulation of autophagy by

herpesvirus Bcl-2 homologs. Autophagy *4*, 268-272.

Liang, C., Feng, P., Ku, B., Dotan, I., Canaani, D., Oh, B.H., and Jung, J.U. (2006). Autophagic and tumour suppressor activity of a novel Beclin1-binding protein UVRAG. Nat Cell Biol *8*, 688-699.

Liang, C., Lee, J.S., Inn, K.S., Gack, M.U., Li, Q., Roberts, E.A., Vergne, I., Deretic, V., Feng, P., Akazawa, C., *et al.* (2008b). Beclin1-binding UVRAG targets the class C Vps complex to coordinate autophagosome maturation and endocytic trafficking. Nat Cell Biol *10*, 776-787.

Liang, X.H., Jackson, S., Seaman, M., Brown, K., Kempkes, B., Hibshoosh, H., and Levine, B. (1999). Induction of autophagy and inhibition of tumorigenesis by beclin 1. Nature *402*, 672-676.

Lim, J., Kim, H.W., Youdim, M.B., Rhyu, I.J., Choe, K.M., and Oh, Y.J. (2011). Binding preference of p62 towards LC3-ll during dopaminergic neurotoxin-induced impairment of autophagic flux. Autophagy *7*, 51-60.

Liu, X., Gal, J., and Zhu, H. (2012). Sequestosome 1/p62: a multi-domain protein with multi-faceted functions. Front Biol *7*, 189-201.

Mair, W., Goymer, P., Pletcher, S.D., and Partridge, L. (2003). Demography of dietary restriction and death in Drosophila. Science *301*, 1731-1733.

Maiuri, M.C., Le Toumelin, G., Criollo, A., Rain, J.C., Gautier, F., Juin, P., Tasdemir, E., Pierron, G., Troulinaki, K., Tavernarakis, N., *et al.* (2007). Functional and physical interaction between Bcl-X(L) and a BH3-like domain in Beclin-1. EMBO J *26*, 2527-2539.

Marino, G., Salvador-Montoliu, N., Fueyo, A., Knecht, E., Mizushima, N., and Lopez-Otin, C. (2007). Tissue-specific autophagy alterations and increased tumorigenesis in mice deficient in Atg4C/autophagin-3. J Biol Chem *282*, 18573-18583.

Martin, P., Diaz-Meco, M.T., and Moscat, J. (2006). The signaling adapter p62 is an important mediator of T helper 2 cell function and allergic airway inflammation. EMBO J *25*, 3524-3533.

Massey, A., Kiffin, R., and Cuervo, A.M. (2004). Pathophysiology of chaperone-mediated autophagy. Int J Biochem Cell Biol *36*, 2420-2434.

Mathew, R., Karantza-Wadsworth, V., and White, E. (2007). Role of autophagy in cancer. Nat Rev Cancer *7*, 961-967.

Matsui, Y., Takagi, H., Qu, X., Abdellatif, M., Sakoda, H., Asano, T., Levine, B., and Sadoshima, J. (2007). Distinct roles of autophagy in the heart during ischemia and reperfusion: roles of AMP-activated protein kinase and Beclin 1 in mediating autophagy. Circ Res *100*, 914-922.

Matsumoto, G., Wada, K., Okuno, M., Kurosawa, M., and Nukina, N. (2011). Serine 403 phosphorylation of p62/SQSTM1 regulates selective autophagic clearance of ubiquitinated proteins. Mol Cell *44*, 279-289.

Matsunaga, K., Saitoh, T., Tabata, K., Omori, H., Satoh, T., Kurotori, N., Maejima, I., Shirahama-Noda, K., Ichimura, T., Isobe, T., *et al.* (2009). Two Beclin 1-binding proteins, Atg14L and Rubicon, reciprocally regulate autophagy at different stages. Nat Cell Biol *11*, 385-396.

Matsuura, A., Tsukada, M., Wada, Y., and Ohsumi, Y. (1997). Apg1p, a novel protein kinase required for the autophagic process in Saccharomyces cerevisiae. Gene *192*, 245-250.

Melendez, A., Talloczy, Z., Seaman, M., Eskelinen, E.L., Hall, D.H., and Levine, B. (2003). Autophagy genes are essential for dauer development and life-span extension in C. elegans. Science *301*, 1387-1391.

Mestre, M.B., Fader, C.M., Sola, C., and Colombo, M.I. (2010). Alpha-hemolysin is required for the activation of the autophagic pathway in Staphylococcus aureus-infected cells. Autophagy *6*, 110-125.

Midorikawa, R., Yamamoto-Hino, M., Awano, W., Hinohara, Y., Suzuki, E., Ueda, R., and Goto, S. (2010). Autophagy-dependent rhodopsin degradation prevents retinal degeneration in Drosophila. J Neurosci *30*, 10703-10719.

Mizushima, N. (2007). Autophagy: process and function. Genes Dev *21*, 2861-2873.

Mizushima, N. (2010). The role of the Atg1/ULK1 complex in autophagy regulation. Curr Opin Cell Biol *22*, 132-139.

Mizushima, N., Kuma, A., Kobayashi, Y., Yamamoto, A., Matsubae, M., Takao, T., Natsume, T., Ohsumi, Y., and Yoshimori, T. (2003). Mouse Apg16L, a novel WD-repeat protein, targets to the autophagic isolation membrane with the Apg12-Apg5 conjugate. J Cell Sci *116*, 1679-1688.

Mizushima, N., Levine, B., Cuervo, A.M., and Klionsky, D.J. (2008). Autophagy fights disease through cellular self-digestion. Nature *451*, 1069-1075.

Nakai, A., Yamaguchi, O., Takeda, T., Higuchi, Y., Hikoso, S., Taniike, M., Omiya, S.,

Mizote, I., Matsumura, Y., Asahi, M., *et al.* (2007). The role of autophagy in cardiomyocytes in the basal state and in response to hemodynamic stress. Nat Med *13*, 619-624.

Nedjic, J., Aichinger, M., Emmerich, J., Mizushima, N., and Klein, L. (2008). Autophagy in thymic epithelium shapes the T-cell repertoire and is essential for tolerance. Nature *455*, 396-400.

Nelson, M.P., and Shacka, J.J. (2013). Autophagy Modulation in Disease Therapy: Where Do We Stand? Curr Pathobiol Rep *1*, 239-245.

Nimmerjahn, F., Milosevic, S., Behrends, U., Jaffee, E.M., Pardoll, D.M., Bornkamm, G.W., and Mautner, J. (2003). Major histocompatibility complex class II-restricted presentation of a cytosolic antigen by autophagy. Eur J Immunol *33*, 1250-1259.

Pattingre, S., Tassa, A., Qu, X., Garuti, R., Liang, X.H., Mizushima, N., Packer, M., Schneider, M.D., and Levine, B. (2005). Bcl-2 antiapoptotic proteins inhibit Beclin 1-dependent autophagy. Cell *122*, 927-939.

Perelman, B., Dafni, N., Naiman, T., Eli, D., Yaakov, M., Feng, T.L., Sinha, S., Weber, G., Khodaei, S., Sancar, A., *et al.* (1997). Molecular cloning of a novel human gene encoding a 63-kDa protein and its sublocalization within the 11q13 locus. Genomics *41*, 397-405.

Petersen, M., Hofius, D., and Andersen, S.U. (2014). Signaling unmasked: Autophagy and catalase promote programmed cell death. Autophagy *10*.

Piras, A., Gianetto, D., Conte, D., Bosone, A., and Vercelli, A. (2011). Activation of

autophagy in a rat model of retinal ischemia following high intraocular pressure. PLoS One *6*, e22514.

Polager, S., Ofir, M., and Ginsberg, D. (2008). E2F1 regulates autophagy and the transcription of autophagy genes. Oncogene *27*, 4860-4864.

Polson, H.E., de Lartigue, J., Rigden, D.J., Reedijk, M., Urbe, S., Clague, M.J., and Tooze, S.A. (2010). Mammalian Atg18 (WIPI2) localizes to omegasome-anchored phagophores and positively regulates LC3 lipidation. Autophagy *6*.

Rabinowitz, J.D., and White, E. (2010). Autophagy and metabolism. Science *330*, 1344-1348.

Randow, F., and Munz, C. (2012). Autophagy in the regulation of pathogen replication and adaptive immunity. Trends Immunol *33*, 475-487.

Ravikumar, B., Duden, R., and Rubinsztein, D.C. (2002). Aggregate-prone proteins with polyglutamine and polyalanine expansions are degraded by autophagy. Hum Mol Genet *11*, 1107-1117.

Rich, K.A., Burkett, C., and Webster, P. (2003). Cytoplasmic bacteria can be targets for autophagy. Cell Microbiol *5*, 455-468.

Rodriguez-Muela, N., Germain, F., Marino, G., Fitze, P.S., and Boya, P. (2012). Autophagy promotes survival of retinal ganglion cells after optic nerve axotomy in mice. Cell Death Differ *19*, 162-169.

Rubinsztein, D.C. (2006). The roles of intracellular protein-degradation pathways in neurodegeneration. Nature *443*, 780-786.

Russell, R.C., Tian, Y., Yuan, H., Park, H.W., Chang, Y.Y., Kim, J., Kim, H., Neufeld, T.P., Dillin, A., and Guan, K.L. (2013). ULK1 induces autophagy by phosphorylating Beclin-1 and activating VPS34 lipid kinase. Nat Cell Biol *15*, 741-750.

Russo, R., Berliocchi, L., Adornetto, A., Varano, G.P., Cavaliere, F., Nucci, C., Rotiroti, D., Morrone, L.A., Bagetta, G., and Corasaniti, M.T. (2011). Calpain-mediated cleavage of Beclin-1 and autophagy deregulation following retinal ischemic injury in vivo. Cell Death Dis *2*, e144.

Rusten, T.E., and Stenmark, H. (2010). p62, an autophagy hero or culprit? Nat Cell Biol *12*, 207-209.

Saftig, P., Tanaka, Y., Lullmann-Rauch, R., and von Figura, K. (2001). Disease model: LAMP-2 enlightens Danon disease. Trends Mol Med *7*, 37-39.

Sahu, R., Kaushik, S., Clement, C.C., Cannizzo, E.S., Scharf, B., Follenzi, A., Potolicchio, I., Nieves, E., Cuervo, A.M., and Santambrogio, L. (2011). Microautophagy of cytosolic proteins by late endosomes. Dev Cell *20*, 131-139.

Sanz, L., Diaz-Meco, M.T., Nakano, H., and Moscat, J. (2000). The atypical PKC-interacting protein p62 channels NF-kappaB activation by the IL-1-TRAF6 pathway. EMBO J *19*, 1576-1586.

Schmid, D., and Munz, C. (2007). Innate and adaptive immunity through autophagy. Immunity *27*, 11-21.

Schweers, R.L., Zhang, J., Randall, M.S., Loyd, M.R., Li, W., Dorsey, F.C., Kundu, M., Opferman, J.T., Cleveland, J.L., Miller, J.L., *et al.* (2007). NIX is required

for programmed mitochondrial clearance during reticulocyte maturation. Proc Natl Acad Sci U S A *104*, 19500-19505.

Scott, R.C., Juhasz, G., and Neufeld, T.P. (2007). Direct induction of autophagy by Atg1 inhibits cell growth and induces apoptotic cell death. Curr Biol *17*, 1-11.

Shi, Y.H., Ding, Z.B., Zhou, J., Hui, B., Shi, G.M., Ke, A.W., Wang, X.Y., Dai, Z., Peng, Y.F., Gu, C.Y., *et al.* (2011). Targeting autophagy enhances sorafenib lethality for hepatocellular carcinoma via ER stress-related apoptosis. Autophagy *7*, 1159-1172.

Shin, J. (1998). P62 and the sequestosome, a novel mechanism for protein metabolism. Arch Pharm Res *21*, 629-633.

Singh, R., and Cuervo, A.M. (2011). Autophagy in the cellular energetic balance. Cell Metab *13*, 495-504.

Singh, R., Kaushik, S., Wang, Y., Xiang, Y., Novak, I., Komatsu, M., Tanaka, K., Cuervo, A.M., and Czaja, M.J. (2009). Autophagy regulates lipid metabolism. Nature *458*, 1131-1135.

Song, Z., An, L., Ye, Y., Wu, J., Zou, Y., He, L., and Zhu, H. (2014). Essential role for UVRAG in autophagy and maintenance of cardiac function. Cardiovasc Res *101*, 48-56.

Starr, T.K., Jameson, S.C., and Hogquist, K.A. (2003). Positive and negative selection of T cells. Annu Rev Immunol *21*, 139-176.

Sun, W.L., Chen, J., Wang, Y.P., and Zheng, H. (2011). Autophagy protects breast cancer cells from epirubicin-induced apoptosis and facilitates

epirubicin-resistance development. Autophagy *7*, 1035-1044.

Takahashi, Y., Coppola, D., Matsushita, N., Cualing, H.D., Sun, M., Sato, Y., Liang, C., Jung, J.U., Cheng, J.Q., Mule, J.J., *et al.* (2007). Bif-1 interacts with Beclin 1 through UVRAG and regulates autophagy and tumorigenesis. Nat Cell Biol *9*, 1142-1151.

Tanaka, Y., Guhde, G., Suter, A., Eskelinen, E.L., Hartmann, D., Lullmann-Rauch, R., Janssen, P.M., Blanz, J., von Figura, K., and Saftig, P. (2000). Accumulation of autophagic vacuoles and cardiomyopathy in LAMP-2-deficient mice. Nature *406*, 902-906.

Taneike, M., Yamaguchi, O., Nakai, A., Hikoso, S., Takeda, T., Mizote, I., Oka, T., Tamai, T., Oyabu, J., Murakawa, T., *et al.* (2010). Inhibition of autophagy in the heart induces age-related cardiomyopathy. Autophagy *6*, 600-606.

Tanida, I. (2011). Autophagosome formation and molecular mechanism of autophagy. Antioxid Redox Signal *14*, 2201-2214.

Tannous, P., Zhu, H., Johnstone, J.L., Shelton, J.M., Rajasekaran, N.S., Benjamin, I.J., Nguyen, L., Gerard, R.D., Levine, B., Rothermel, B.A., *et al.* (2008). Autophagy is an adaptive response in desmin-related cardiomyopathy. Proc Natl Acad Sci U S A *105*, 9745-9750.

Tey, S.K., and Khanna, R. (2012). Host immune system strikes back: autophagy-mediated antigen presentation bypasses viral blockade of the classic MHC class I processing pathway. Autophagy *8*, 1839-1841.

Thoresen, S.B., Pedersen, N.M., Liestol, K., and Stenmark, H. (2010). A

phosphatidylinositol 3-kinase class III sub-complex containing VPS15, VPS34, Beclin 1, UVRAG and BIF-1 regulates cytokinesis and degradative endocytic traffic. Exp Cell Res *316*, 3368-3378.

Tolkovsky, A.M. (2009). Mitophagy. Biochim Biophys Acta *1793*, 1508-1515.

Tong, J., Yan, X., and Yu, L. (2010). The late stage of autophagy: cellular events and molecular regulation. Protein Cell *1*, 907-915.

Tuttle, D.L., Lewin, A.S., and Dunn, W.A., Jr. (1993). Selective autophagy of peroxisomes in methylotrophic yeasts. Eur J Cell Biol *60*, 283-290.

Vadlamudi, R.K., Joung, I., Strominger, J.L., and Shin, J. (1996). p62, a phosphotyrosine-independent ligand of the SH2 domain of p56lck, belongs to a new class of ubiquitin-binding proteins. J Biol Chem *271*, 20235-20237.

Vanhaesebroeck, B., Guillermet-Guibert, J., Graupera, M., and Bilanges, B. (2010). The emerging mechanisms of isoform-specific PI3K signalling. Nat Rev Mol Cell Biol *11*, 329-341.

Veenhuis, M., Salomons, F.A., and Van Der Klei, I.J. (2000). Peroxisome biogenesis and degradation in yeast: a structure/function analysis. Microsc Res Tech *51*, 584-600.

Wang, R.C., Wei, Y., An, Z., Zou, Z., Xiao, G., Bhagat, G., White, M., Reichelt, J., and Levine, B. (2012). Akt-mediated regulation of autophagy and tumorigenesis through Beclin 1 phosphorylation. Science *338*, 956-959.

Wang, X., Osinska, H., Klevitsky, R., Gerdes, A.M., Nieman, M., Lorenz, J., Hewett, T., and Robbins, J. (2001). Expression of R120G-alphaB-crystallin causes

aberrant desmin and alphaB-crystallin aggregation and cardiomyopathy in mice. Circ Res *89*, 84-91.

Webb, J.L., Ravikumar, B., Atkins, J., Skepper, J.N., and Rubinsztein, D.C. (2003). Alpha-Synuclein is degraded by both autophagy and the proteasome. J Biol Chem *278*, 25009-25013.

Wei, Y., Zou, Z., Becker, N., Anderson, M., Sumpter, R., Xiao, G., Kinch, L., Koduru, P., Christudass, C.S., Veltri, R.W., *et al.* (2013). EGFR-mediated Beclin 1 phosphorylation in autophagy suppression, tumor progression, and tumor chemoresistance. Cell *154*, 1269-1284.

Weinmann, A.S., Bartley, S.M., Zhang, T., Zhang, M.Q., and Farnham, P.J. (2001). Use of chromatin immunoprecipitation to clone novel E2F target promoters. Mol Cell Biol *21*, 6820-6832.

Winslow, A.R., Chen, C.W., Corrochano, S., Acevedo-Arozena, A., Gordon, D.E., Peden, A.A., Lichtenberg, M., Menzies, F.M., Ravikumar, B., Imarisio, S., *et al.* (2010). alpha-Synuclein impairs macroautophagy: implications for Parkinson's disease. J Cell Biol *190*, 1023-1037.

Wirawan, E., Lippens, S., Vanden Berghe, T., Romagnoli, A., Fimia, G.M., Piacentini, M., and Vandenabeele, P. (2012). Beclin1: a role in membrane dynamics and beyond. Autophagy *8*, 6-17.

Wojcik, S. (2013). Crosstalk between autophagy and proteasome protein degradation systems: possible implications for cancer therapy. Folia Histochem Cytobiol *51*, 249-264.

Wong, E.S., Tan, J.M., Soong, W.E., Hussein, K., Nukina, N., Dawson, V.L., Dawson, T.M., Cuervo, A.M., and Lim, K.L. (2008). Autophagy-mediated clearance of aggresomes is not a universal phenomenon. Hum Mol Genet *17*, 2570-2582.

Yamamoto, A., and Simonsen, A. (2011). The elimination of accumulated and aggregated proteins: a role for aggrephagy in neurodegeneration. Neurobiol Dis *43*, 17-28.

Yang, S., Wang, X., Contino, G., Liesa, M., Sahin, E., Ying, H., Bause, A., Li, Y., Stommel, J.M., Dell'antonio, G., *et al.* (2011). Pancreatic cancers require autophagy for tumor growth. Genes Dev *25*, 717-729.

Yang, Z., Huang, J., Geng, J., Nair, U., and Klionsky, D.J. (2006). Atg22 recycles amino acids to link the degradative and recycling functions of autophagy. Mol Biol Cell *17*, 5094-5104.

Yang, Z., and Klionsky, D.J. (2010). Eaten alive: a history of macroautophagy. Nat Cell Biol *12*, 814-822.

Yin, X., Cao, L., Kang, R., Yang, M., Wang, Z., Peng, Y., Tan, Y., Liu, L., Xie, M., Zhao, Y., *et al.* (2011). UV irradiation resistance-associated gene suppresses apoptosis by interfering with BAX activation. EMBO Rep *12*, 727-734.

Yitzhaki, S., Huang, C., Liu, W., Lee, Y., Gustafsson, A.B., Mentzer, R.M., Jr., and Gottlieb, R.A. (2009). Autophagy is required for preconditioning by the adenosine A1 receptor-selective agonist CCPA. Basic Res Cardiol *104*, 157-167.

Yu, W.H., Cuervo, A.M., Kumar, A., Peterhoff, C.M., Schmidt, S.D., Lee, J.H., Mohan, P.S., Mercken, M., Farmery, M.R., Tjernberg, L.O., *et al.* (2005).

Macroautophagy--a novel Beta-amyloid peptide-generating pathway activated in Alzheimer's disease. J Cell Biol *171*, 87-98.

Zalckvar, E., Berissi, H., Mizrachy, L., Idelchuk, Y., Koren, I., Eisenstein, M., Sabanay, H., Pinkas-Kramarski, R., and Kimchi, A. (2009). DAP-kinase-mediated phosphorylation on the BH3 domain of beclin 1 promotes dissociation of beclin 1 from Bcl-XL and induction of autophagy. EMBO Rep *10*, 285-292.

Zeng, X., Overmeyer, J.H., and Maltese, W.A. (2006). Functional specificity of the mammalian Beclin-Vps34 PI 3-kinase complex in macroautophagy versus endocytosis and lysosomal enzyme trafficking. J Cell Sci *119*, 259-270.

Zhao, Z., Ni, D., Ghozalli, I., Pirooz, S.D., Ma, B., and Liang, C. (2012a). UVRAG: at the crossroad of autophagy and genomic stability. Autophagy *8*, 1392-1393.

Zhao, Z., Oh, S., Li, D., Ni, D., Pirooz, S.D., Lee, J.H., Yang, S., Lee, J.Y., Ghozalli, I., Costanzo, V., *et al.* (2012b). A dual role for UVRAG in maintaining chromosomal stability independent of autophagy. Dev Cell *22*, 1001-1016.

Zhong, Y., Wang, Q.J., Li, X., Yan, Y., Backer, J.M., Chait, B.T., Heintz, N., and Yue, Z. (2009). Distinct regulation of autophagic activity by Atg14L and Rubicon associated with Beclin 1-phosphatidylinositol-3-kinase complex. Nat Cell Biol *11*, 468-476.

Zhu, H., Tannous, P., Johnstone, J.L., Kong, Y., Shelton, J.M., Richardson, J.A., Le, V., Levine, B., Rothermel, B.A., and Hill, J.A. (2007). Cardiac autophagy is a maladaptive response to hemodynamic stress. J Clin Invest *117*, 1782-1793.